UNIVERSITÄTSKLINIKUM HAMBURG-EPPENDORF

Zentrum für Diagnostik / Institut für Neuropathologie

Direktor Prof. Dr. med. Markus Glatzel

An investigation of interaction between Neuroserpin and its putative targets PC1/3, PC2 and Furin with a YFP-protein complementation assay

Dissertation

zur Erlangung des Grades eines Doktors der Medizin
an der Medizinischen Fakultät der Universität Hamburg.

vorgelegt von:

Felix Johannes Alfred Wiesmüller
aus Regensburg

Hamburg 2015

Angenommen von der
Medizinischen Fakultät der Universität Hamburg am: 07.12.2015

Veröffentlicht mit Genehmigung der
Medizinischen Fakultät der Universität Hamburg.

Prüfungsausschuss, der/die Vorsitzende: **Prof. Dr. Markus Glatzel**

Prüfungsausschuss, zweite/r Gutachter/in: **Prof. Dr. Hans-Jürgen Kreienkamp**

Prüfungsausschuss, dritte/r Gutachter/in:

Index

1 Introduction

1.1 Neuroserpin

1.1.1 Discovery

Neuroserpin first was described in 1989 in chicken dorsal root ganglia by Stoeckli, Lemkin et al. (1989). In their screening experiment they used a Campenot chamber (Campenot 1977) to perform metabolic labeling of proteins specifically secreted by axons. A two-dimensional SDS-PAGE revealed two novel proteins of 132-140kDa and 54-60kDa, the latter being coined "axonin-2". Osterwalder, Contartese et al. (1996), were the first to perform amino acids microsequencing from purified chicken ocular vitreous fluid axonin-2. Thereafter, a full-length cDNA from chicken brain cDNA library was obtained. Comparative searches in gene databases identified axonin-2 as a member of the serpin family. Since they had found this 55kDa protein to be expressed in the central nervous system (CNS) and the peripheral nervous system (PNS), they renamed it "neuroserpin". Amplifications from human and murine cDNA libraries showed that neuroserpin differed greatly from other known mammalian serpins with the closest match to their amino acid sequence being nexin-1 (PN-1) and plasminogen activator inhibitor-1 (PAI-1). Ultimately, researchers started to closely investigate the properties of neuroserpin. PN-1 and PAI-1 were also known as inhibitors of tissue-type plasminogen activator (tPA). Eventually, it did not take long to prove that neuroserpin inhibits tPA in vitro, as well as further defining its chromosomal and tissue localization (Hastings, Coleman et al. 1997; Krueger, Ghisu et al. 1997; Schrimpf, Bleiker et al. 1997). In 1999, the groundbreaking discovery of mutant neuroserpin polymers causing familial dementia by Davis was published in the Nature Journal (Davis, Shrimpton et al. 1999). Meanwhile, studies continue to yield new links and properties of the protein, the latest being its involvement in brain metastasis growth (Valiente, Obenauf et al. 2014).

1.1.2 Serpin Family and Serpin kinetics

"The serpins (<u>ser</u>ine <u>p</u>roteinase <u>inhibitors</u>) are a superfamily of proteins (350-500 amino acids in size) that fold into a conserved structure and employ a unique suicide substrate-like inhibitory mechanism"
(Silverman, Bird et al. 2001, p.33293).

This superfamily comprises about 500 serpins which can be divided into 16 clades (Irving, Pike et al. 2000). Most serpins inhibit serine proteinases of the chymotrypsin family, while some are targeted against other enzymes or are involved in hormone transport or blood pressure regulation (Silverman, Bird et al. 2001). Serpins are distributed among eukaryotes, viruses, and some prokaryotes (Irving, Steenbakkers et al. 2002). They have not been found in fungi and chlorophytes with the exception of some higher plants (Gettins 2002). All serpins exhibit a conserved structure containing β-sheets A, B and C and at least 7 α-helices of approximately 350 amino acids, as well as a reactive center loop (RCL) between β-sheets A and C. Within this conserved structure there are so-called conserved residues of approximately 50 amino acids which comprise the hydrophobic core of the protein (Silverman, Bird et al. 2001).

According to Olson and Gettins (2011), they studied how serpins underwent different conformational states. For example, in the latent state, the RCL, C-terminally anchored at β-sheet C, has been removed from its sheet C and is C-terminally inserted into β-sheet A. However, under physiologic conditions the conformational change to the latent state does not occur. While in the cleaved state, the RCL has undergone cleavage and is N-terminally inserted into the β-sheet A instead. In the δ-conformation, mutations at the shutter region, a site located at the end of sheet A that controls the opening of the sheet, induce the RCL to lose interaction with sheet C and be partially inserted into the proximal sheet A. The F helix is then unwound and inserted in the distal end of sheet A. Ultimately, the δ-conformation induces polymer formation by linking RCL-A sheets with RCL-C sheets.
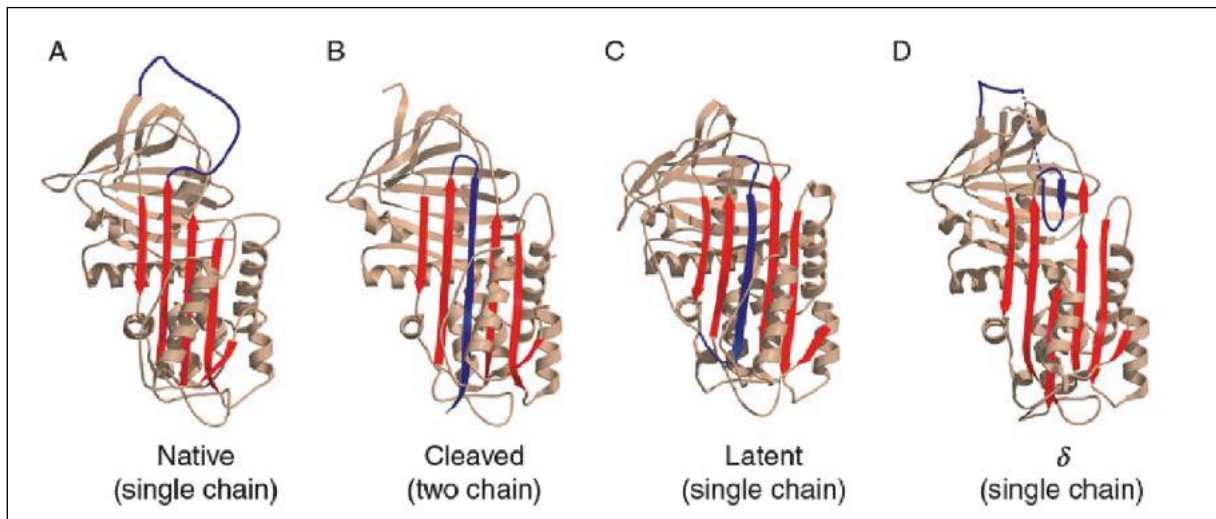
Figure 1.1: Ribbon presentation of different conformational states of serpins. X-ray structures of α₁PI (α₁-proteinase inhibitor) in its native serpin state (A) and in the cleaved state (B). Latent state of PAI-1 (plasminogen activator inhibitor-1)(C). δ-conformation of α₁-antichymotrypsin L55P variant (D). (RCL=blue, β-sheet A=red, other=gray)
Adopted from (Olson and Gettins 2011).

In 2008, Yamasaki, Li et al. proposed a novel polymerization model where two antiparallel β-strands of one serpin to insert into the center of the principal β-sheet of another serpin.
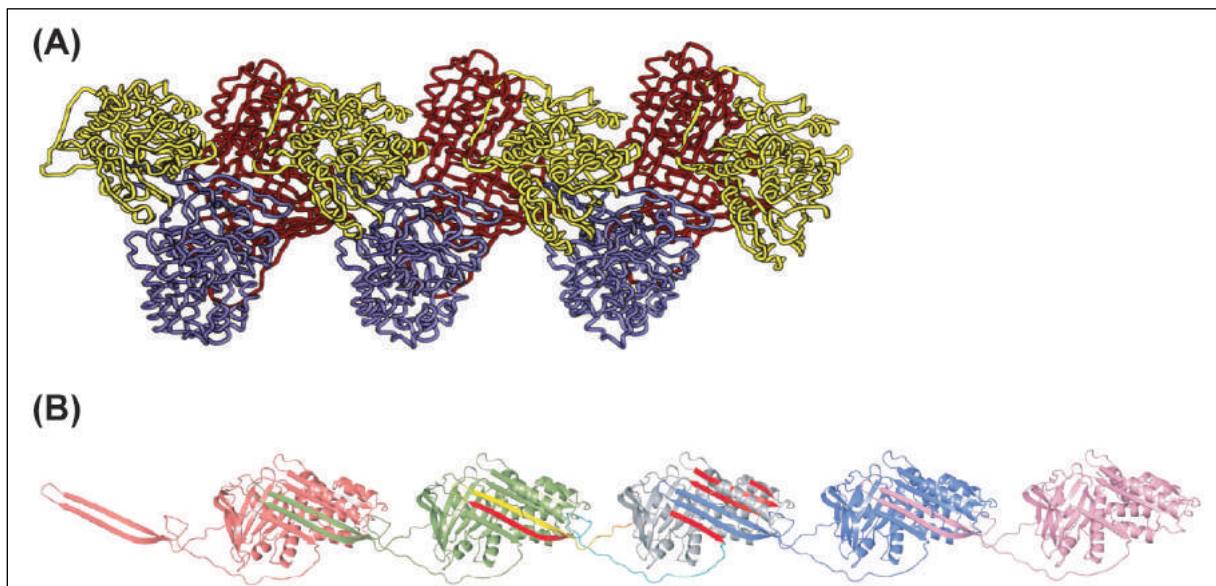
Figure 1.2: Proposed serpin polymers. Traditional loop-sheet model as described by Elliott, Lomas et al. (1996). RCLs are inserted into β-sheets A (A). Novel model of antiparallel β-sheet insertion described by Yamasaki, Li et al. (2008) (B). Description and images adopted from (Olson and Gettins 2011).

A unique feature of the serpin family is their inhibitory mechanism through an irreversible suicide substrate formed by the serpin and the target protein within a branched pathway (figure 1.3) (Olson and Gettins 2011). A serine or cysteine protease recognizes specific

residues that are exposed by the RCL of the serpin and noncovalently binds to them. Moreover, there may be exosites or other cofactors, such as heparin that facilitate the binding process leading to the formation of a Michaelis-like complex. The RCL is subsequently cleaved at the scissile peptide bond by the protease. However, the protease cannot dissociate immediately, as an acyl-enzyme intermediate results upon cleavage where the protease is covalently bound to the serpin. The cleavage allows the serpin to undergo a conformational change and the bound protease is translocated by more than 70Å from the top of the serpin to its bottom. If the protease is able to hydrolize the bond within the time window of translocation, it can dissociate. However, if it is fully translocated, it is pushed against the bottom of the serpin, distorting the active site of the protease where it becomes kinetically trapped. Still, noncatalyzed hydrolysis may occur, thus yielding a fully functional protease and a cleaved serpin, although the rate of dissociation of a trapped protease (k_5) is many orders of magnitudes less than the substrate-protease reaction (Olson and Gettins 2011).
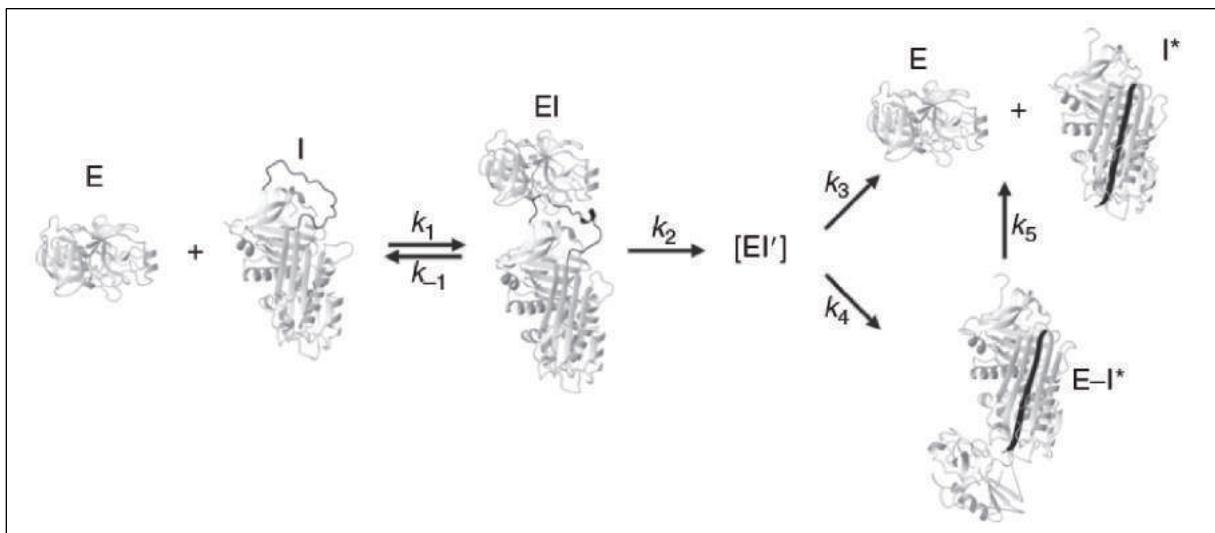
*Figure 1.3: Serpin suicide substrate mechanism as depicted by the reaction of the serpin α₁PI (**I**) and the protease trypsin (**E**). The protease binds to the reactive center loop (RCL) of the serpin with the second-order rate constant k_1, forming a noncovalent Michaelis-like complex (**EI**). Dissociation of the complex is possible at a rate of k_{-1}, but since $k_2 >> k_{-1}$ an acyl-enzyme intermediate (**EI'**) is formed by cleavage of the scissile peptide bond at a rate of k_2. In this intermediate, the protease is covalently bound to the cleaved peptide carbonyl and dragged from the top to the bottom of the β-sheet A (indicated by black coloring), as the RCL partially inserts into it. From there, it can end up kinetically trapped (**E-I***) by complete insertion of RCL into β-sheet A at rate of k_4. If hydrolysis is completed before E-I* can be formed, then the cleaved serpin and the protease dissociate at a rate of k_3. Still, noncatalyzed hydrolysis may occur at a rate of k_5, leading to free products, as well.*
Description according to (Olson and Gettins 2011), image adopted from (Dobo and Gettins 2004).

Due to the possibility of the protease escaping the kinetic trap by hydrolyzing the bond of the acyl-enzyme complex, the pathway of the serpin inhibitory mechanism is branched. One branch leads to dissociation of the acyl-enzyme intermediate by swift hydrolysis with a rate

order of (k_3). The other branch is favored by an energy difference of approx. 60kcal mol^{-1}, leading to a conformational change and distorting the serpine with a rate order of (k_4). Rate orders are specific to each combination of serpin and different target proteases. Therefore, each combination has an intrinsic efficiency, depending on the overall rates of the branched pathways (Olson and Gettins 2011).

"This efficiency is defined as the stoichiometry of inhibition (SI), which is the number of molecules of serpin required to inhibit one molecule of protease and represents the inverse of the fraction of the first-formed acyl-intermediate that ends up as trapped complex" (Olson and Gettins 2011, p.199).

The SI has been defined by Patston, Gettins et al. (1991) as the following:

$$SI = (k_3 + k_4)/ k_4$$

Serpin-protease complexes are internalized via clathrin-coated pits by binding to receptors of the low-density lipoprotein (LDL) receptor family (Olson and Gettins 2011). In the case of neuroserpin, the low-density lipoprotein receptor-related protein (LRP) seems to play a role in regulating neuroserpin levels by internalizing active neuroserpin, as well as neuroserpin-tPA complexes (Makarova, Mikhailenko et al. 2003). Generally, native and cleaved serpins can be cleared from circulation. Yet, their half-lives are significantly longer than those of complexes (Olson and Gettins 2011).

1.1.3 Neuroserpin gene and regulation of expression

Human neuroserpin, or "SERPINI1" (Silverman, Bird et al. 2001), is located on chromosome 3 at position 3q26 (Schrimpf, Bleiker et al. 1997). It consists of an open reading frame of over 1230bp with a 5' untranslated region (UTR) of 81 nucleotides and a 3' UTR of 248 nucleotides. Between nucleotides 1535 and 1540 there is a putative polyadenylation signal AATAAA. In contrast, the mouse gene presents two polyadenylation sites. Yet, alternative polydenylation is suspected to occur in human neuroserpin which would explain the different sizes of mRNA and isolated cDNA clone (Galliciotti and Sonderegger 2006). Translation starts in exon 2 and ends in exon 9. A TATA-less promoter with two Sp1 sites (transcription factor) and an Inr sequence (Inr-binding protein), both responsible for initiation of transcription, has been identified. A CAAT-box at position -65 is thought to be involved in binding trans-activating factors for transcription of the neuroserpin gene. Overlapping with

the Sp1 sites are two AP-2 binding sites that are thought to play a role during embryogenesis. Furthermore, there are binding sites for transcription factors zif/268, olf-1, and TEF, a thyrotroph embryonic factor of the family of leucine zippers. (Berger, Kozlov et al. 1998)

Located approx. 100kb apart from SERPINI1 on 3q26 is SERPINI2 (Pancpin). Instead of 9 exons and 8 introns, it consists of 8 exons and 7 introns, indicating that it may not have evolved from the same family as neuroserpin. The distribution of expression levels within the body (mainly in the pancreas), as well as associated diseases (pancreatic insufficiency) also differ from those of neuroserpin (Chang, Chang et al. 2000).

Berger, Kozlov et al. (1999) reported that the transcription of neuroserpin mRNA is increased in hippocampal neurons by depolarization as simulated with elevated extracellular concentrations of KCl. The increase of mRNA was observed in a late phase, eight hours after exposure to KCl. Zif/268, a zinc finger protein, suppresses neuroserpin activity by binding to its promoter. Since zif/268 is known as an immediate early gene, induced by neuronal electrical activity, it may operate as silencer during the early phase. This would provide a target protease time to catabolize during the early phase and upon fulfilling its task, be terminated by neuroserpin binding during the late phase. (Galliciotti and Sonderegger 2006)

HuD, a RNA-binding protein from the Elav-like (embrionic lethal abnormal vision) family is believed to regulate neuroserpin post-transcriptionally. Three HuD binding sequences in the 3'-UTR of neuroserpin have been identified and *in vitro* binding has been observed in PC12 cells. Likewise, HuD protein and neuroserpin mRNA co-localize in the same rat brain areas, namely hippocampus, cerebral cortex and olfactory bulb, in which no other Elav-like proteins are expressed (Okano and Darnell 1997; Cuadrado, Navarro-Yubero et al. 2002).

Binding of HuD to neuroserpin RNA prolongs its lifetime, leading to increased levels of neuroserpin protein. Since HuD expression is restrained by thyroid hormone T3 (Cuadrado, Navarro-Yubero et al. 2003), concentrations of neuroserpin protein are indirectly controlled by T3 on an RNA level (Navarro-Yubero, Cuadrado et al. 2004).

1.1.4 3D Crystal Structure

Phylogenically, neuroserpin separated from other serpins at an early stage with many residues deviating from otherwise highly conserved positions within the serpin superfamily (Irving, Pike et al. 2000; Takehara, Onda et al. 2009). In 2001, Briand, Kozlov et al. published the crystal structure of cleaved murine neuroserpin. A 2.1Å crystal structure of human neuroserpin (Fig. 1.4B) was reported in 2009 by Takehara, Onda et al.. The overall fold was found to be very similar to that of α_1-antitrypsin with a root-mean-square deviation (r.m.s.d.) of 1.8Å with 322 equivalent C^{α} residues. Different from the antitrypsin structure is the RCL that resembles a 3_{10} helix. This is a unique finding since a helical RCL has been mainly reported in two loop swap variants of serpins. Likewise, an acidic cluster has been detected over large portions of neuroserpin, suggesting that positively charged cofactors are involved in activity, transport and degradation of neuroserpin (Fig. 1.4A). Another unique property is an omega loop between strands 1B and 2B that bulges out of the molecule. Additional experiments concludet that the omega loop "may be important in the interaction between neuroserpin and tPA" (Takehara, Onda et al. 2009, p.16). By including mutant S340A neuroserpin in their investigation, they discovered that the addition of only one oxygen atom to the residue at position 340 causes a major instability of the shutter region, ultimately leading to polymerization. This finding accentuates the proneness of this serpin to form polymers.

Subsequently, Ricagno, Caccia et al. (2009) studied the crystal structure of native and cleaved neuroserpin where they reported that the C-D helix region binded to an unknown ligand.
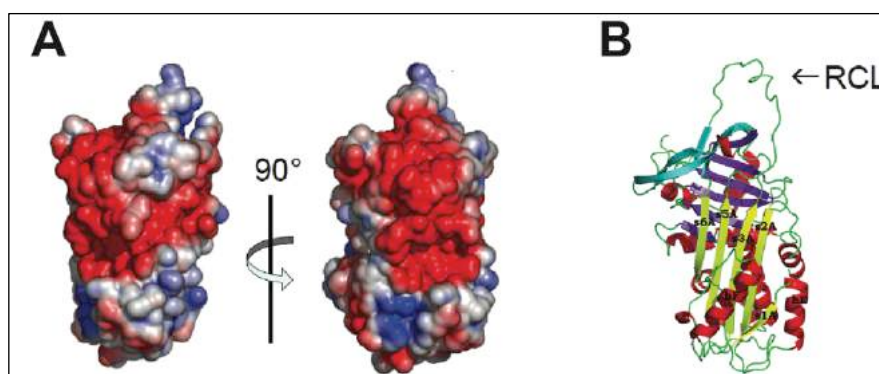
Figure 1.4: (A) Electrostatic surface of human neuroserpin illustrating large areas of acidic clusters (blue=positive, red=negative).
(B) Cartoon of native human neuroserpin displaying typical serpin fold, including the reactive center loop (RCL) (sheet A=yellow, sheet B=blue, sheet C=cyan, helices=red, loops=green);
(A) adopted and modified from (Takehara, Onda et al. 2009), (B) adopted and modified from (Ricagno, Caccia et al. 2009).

1.1.5 Tissue distribution

Expression of neuroserpin is initiated during migration of neurons at an embryonic stage. In the mouse, presence of neuroserpin RNA has been detected at E14. From then on, the amount of protein was noticed to increase, reaching its highest concentration perinatally. Thereafter, amounts decreased, reaching an intermediate level in the adult mouse (Fig. 1.5). During development (E15 and older), highest levels were measured in neocortex, hippocampus, cerebellar primordium, pons and medulla. Other than in the CNS, murine RNA has also been detected in the dorsal root ganglia of the PNS, vegetative ganglia, cranial nerve ganglia, olfactory epithelium, and the liver during early development (Krueger, Ghisu et al. 1997). During development of the human embryo, neuroserpin RNA has been traced in the brain and at lower levels in the fetal liver and kidney (Hastings, Coleman et al. 1997).
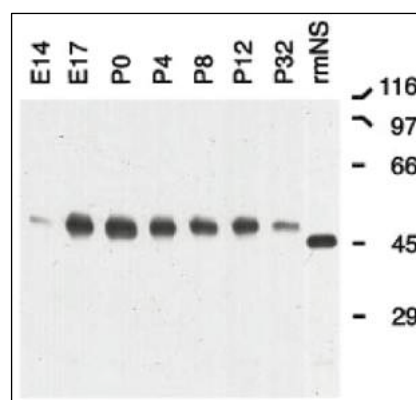
Figure 1.5: Immunoprecipitation of murine brain extracts displaying neuroserpin levels at different developmental stages. Highest concentration of neuroserpin RNA is detected perinatally (P0).
Image adopted from (Krueger, Ghisu et al. 1997);
description according to (Krueger, Ghisu et al. 1997).

In the adult human, neuroserpin RNA localizes strongly in the brain, significantly less in the pancreas, and is barely traceable in the testes and in the heart (Fig. 1.6). High levels of neuroserpin message were observed throughout the CNS with the exception of the cerebellum (Hastings, Coleman et al. 1997). *In situ* hybridization also showed RNA to be present in the pituitary gland and the medulla of the adrenal gland (Hill, Parmar et al. 2000).
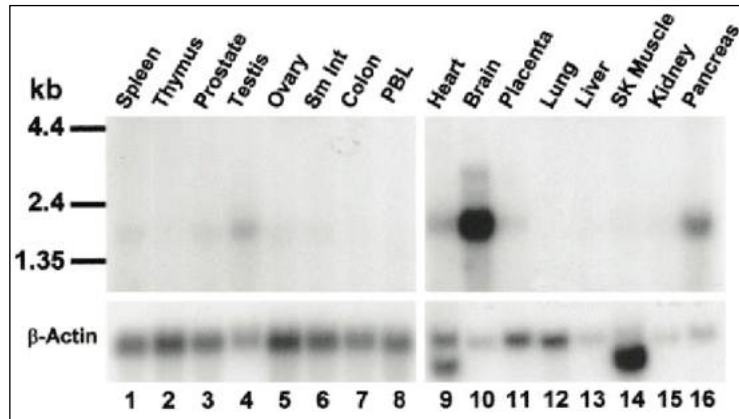
Figure 1.6: Northern blot analysis of neuroserpin RNA from various adult human tissues. RNA is mainly detected in the brain and, to smaller amounts, the pancreas, the testis, and the heart. Image adopted from (Hastings, Coleman et al. 1997).

Immunhistochemical staining of murine neuronal tissue revealed neuroserpin protein to be confined to neurons. An exception to this is the presence of neuroserpin in ependymal cells of the choroid plexus and cells of the brush border which line the ventricles. Yet, these ependymal cells are thought to be derived from microglial cells. Significant staining was seen in the neurons of the hypothalamus and the cortex, in large motor neurons of the medulla oblongata, and in neurons from the spinal cord, including their axons. Another cell type that stained strongly for the protein were Purkinje cells of the cerebellum (Hastings, Coleman et al. 1997).

Neuroserpin was also found in the human myeloid lineage with the highest levels of neuroserpin mRNA observed in activated dendritic cells (Kennedy, van Diepen et al. 2007).

1.1.6 Cellular localization and trafficking

Hill, Parmar et al. (2000) demonstrated that neuroserpin resides in dense-cored secretory vesicles of endocrine or neuronal tissue. This implies an involvement in the regulated secretion pathway. Moreover, the protein partly proved to be membrane-associated, "suggesting that neuroserpin could also act at the cell surface" (p.599).

Neuroserpin is not stored in the ER or Golgi, but directed to and stored in secretory vesicles. Trafficking is achieved by a sorting signal at the C-terminus consisting of 13 amino acids. Lack of the targeting sequence results in trafficking via the constitutive pathway (Ishigami, Sandkvist et al. 2007).

In primary cortical cultures, active neuroserpin is internalized by lipoprotein receptor-related protein (LRP) or very-low-density lipoprotein (VLDL) receptors and degraded. Neuroserpin

in complex with its target tPA is internalized by LRP, but not VLDL receptors. The endocytosis of the active state is surprising since serpins usually are taken up as complexes. In addition, cleaved neuroserpin is not subjected to endocytosis. The authors concluded that intracellular neuroserpin in the cleaved state must be the result of cell-associated proteolytic degradation (Kounnas, Church et al. 1996; Stefansson, Muhammad et al. 1998; Makarova, Mikhailenko et al. 2003).

1.1.7 Known targets

Neuroserpin is an *in vitro* inhibitor of tPA, urokinase plasminogen activator (uPA), nerve growth factor-γ (NGF-γ), trypsin and plasmin (Hastings, Coleman et al. 1997; Krueger, Ghisu et al. 1997). Complex formation was demonstrated *in vitro* with tPA, uPA, NGF-γ and plasmin, with tPA being the most likely target according to complex stability (Krueger, Ghisu et al. 1997; Osterwalder, Cinelli et al. 1998).

Expression of tPA within the various tissues and cell types of the CNS also correlates with that of neuroserpin (Hastings, Coleman et al. 1997; Teesalu, Kulla et al. 2004). Besides similar tissue distribution, they illustrate another shared characteristic, namely release upon neural depolarization (Qian, Gilbert et al. 1993; Berger, Kozlov et al. 1999). The combined findings of the in vitro complexes and same spatiotemporal distribution of neuroserpin and tPA suggest tPA as the main target of neuroserpin.

Furthermore, *in vivo* inhibition of tPA by neuroserpin was indicated in a study by Cinelli, Madani et al. (2001) involving transgenic mice with overexpressed production of neuroserpin. Zymography of brain homogenates revealed the tPA activity in these mice to be strongly reduced.

Concordant with this observation are the opposing effects of neuroserpin and tPA in pathologic conditions. In the brain, tPA contributes to disruption of neurovascular homeostasis after neurotrauma, leading to edema, inflammation and cell death (Sashindranath, Sales et al. 2012). When tPA was compared to its putative counterpart neuroserpin in models of brain injury, it was discovered that the detrimental effects of tPA were alleviated by the expression of neuroserpin. While tPA promotes neurovascular injury, neuroserpin acts as a neuroprotective by preventing damage (Zhang, Zhang et al. 2002; Gelderblom, Neumann et al. 2013). However, Wu, Echeverry et al. (2010) demonstrated that neuroserpin induces ischemic tolerance independently of tPA. Their findings entirely oppose the forementioned theory of direct inhibition of tPA by neuroserpin.

Moreover, the conclusion of tPA being the primary target of neuroserpin is inconsistent with the stability of neuroserpin-tPA complexes. Interestingly, complexes of neuroserpin and tPA are short-lived *in vitro*, and tPA returns fully active after deacetylation (Barker-Carlson, Lawrence et al. 2002). Time spans of observed complexes vary among the several studies published, but in general are shorter than expected. Osterwalder, Cinelli et al. (1998) reported stable complexes for at least five hours, while Barker-Carlson, Lawrence et al. (2002) stated that complexes are not longer than 80 min for single-chain tPA or 20 min for two-chain tPA at 37°C. Moreover, according to the calculations performed after chromogenic assays by Ricagno, Caccia et al. (2009), a complex formed by neuroserpin and two-chain tPA has a half-life of 10 min. The short-lived nature of these complexes implies that tPA may not be the true target of neuroserpin. Generally, rapid breakdown times are observed in pairs that are not physiologic (Plotnick, Samakur et al. 2002). Indeed, complexes of tPA and NS are less stable than other related complexes found in serpins.

In vivo, high molecular weight complexes positive for neuroserpin have been described (de Groot, Pol et al. 2005). However, until recently the exact composition of the complexes have not been further analysed.

Many functions (discussed later under "known functions") have been attributed to neuroserpin. As a serin proteinase inhibitor, it causes an effect indirectly by decelerating the biocatalytical reaction between proteinase and substrate. The targeted proteinase may act intra- or extracellularly. Both, neuroserpin and tPA, are sorted to the regulated secretory pathway where they localize to dense-cored secretory vesicles before being secreted. Nonetheless, the physiologic pH found in these vesicles of pH 5,0-5,5 is too low to allow complex formation with tPA, which takes place at pH 7,0-7,5 (Parmar, Coates et al. 2002). Therefore, it seems unlikely that any intracellular pathway may be regulated through inhibition of tPA by neuroserpin.

One of the main roles associated with neuroserpin is regulation of cell morphology. However, it has been proven by *in vitro* studies that neuroserpin executes its modulations independently of tPA (Hill, Parmar et al. 2000; Lee, Coates et al. 2008). Another role associated with neuroserpin is the regulation of emotional behavior. In their study, Madani, Kozlov et al. (2003) observed that the involvement of neuroserpin is not influenced by tPA. Zymographic analysis of neuroserpin-deficient mouse brain revealed unchanged enzymatic activity of tPA when compared to the control group. The authors suggested that neuroserpin exerted actions

in vivo independently from tPA. This further supports the hypothesis that tPA may not be the actual target of neuroserpin.

A recent study by Tsang, Young et al. (2014) provided proof of FLAG-neuroserpin forming a complex with tPA *in vivo*. Yet, contrary to reduced tPA activity as described by Cinelli, Madani et al. (2001), Tsang, Young et al. (2014) reported that tPA activity was unaffected by injected neuroserpin and the possibility of a non-inhibitory mechanism could not be excluded. A review on neuroserpin by Galliciotti and Sonderegger (2006) cites several other publications on the topic of tPA complexation. They concluded that "neuroserpin is neither a pure inhibitor, nor a pure substrate of tPA. The profiled neuroserpin inhibition of tPA suggests that it acts like a competitive substrate" (p.37). Research has indicated that there is a general consent of tPA being the true physiological target. Still, scientific evidence is rather contradictory.

1.1.8 Known functions

1.1.8.1 Role in neurogenesis

Several roles in the mammalian body have been attributed to neuroserpin. Since neuroserpin is mainly found in neuronal tissue, these linked functions evolve around the CNS and PNS. The distribution of the protein in embryos, as described by Hastings, Coleman et al. (1997); Krueger, Ghisu et al. (1997), strongly suggests it to be involved in migration and development of neuronal cells and their resulting structures. In addition, neuroserpin is thought to play a role in neurogenesis. This was suggested by Yamada, Takahashi et al. (2010), who analyzed gene expression of rat hippocampi. The hippocampus is a brain structure that belongs to the limbic system. It is responsible for consolidation of short-term to long-term memory and spatial memory (e.g., navigation). The authors provided evidence that neuroserpin is expressed in immature neurons in adult hippocampus. Aside from the established implication in embryonic development, this discovery indicates a role in adult neurogenesis.

1.1.8.2 Role in regeneration

Neuro-restorative qualities are of particular interest for clinical applications. At present, due to the scarce regenerative ability of the nervous system, only symptomatic treatment is recommended for many neurologic conditions like spinal cord injury, stroke, and amyotrophic lateral sclerosis. Nonetheless, cells in the nervous system with restorative capacities exist. Olfactory ensheathing cells (OECs) are a specialized glia cell type contained by olfactory

axons and used extensively for research purposes on axon regeneration (Doucette 1991). Microarray screening in OECs in intact versus lesioned animals revealed SERPINI1 (neuroserpin) expression to be upregulated. SERPINI1 knockdown reduced neurite growth in co-cultured primary dorsal root ganglion (DRG) neurons, while a gain-of-function screen demonstrated enhanced neurite growth. In injured olfactory nerve layer (ONL), neuroserpin expression is upregulated at the 6th day post lesion. Immunostaining of inured ONL at the 6th day post lesion located SERPINI1 especially at the site of guidance by OECs. According to Roet, Franssen et al. (2013), these findings indicate involvement of neuroserpin in the regeneration of neuronal network.

1.1.8.3 Role in neuroendocrine system

In PC12 cells, derived from rat pheochromoctoma (Greene and Tischler 1976), expression of neuroserpin correlates with expression of N-cadherin, and this regulates cell adhesion (Lee, Coates et al. 2008). In a study by Parmar, Coates et al. (2002) using PC12 cells, they identified neuroserpin as a regulator of neurite outgrowth. Similarly, neuroserpin induces extension of neurite-like processes and growth cones in AtT20 cells that are derived from mouse anterior pituitary gland. This may also be interpreted as a part of developmental processes. Hill, Parmar et al. (2000) stated that "the extension of cellular processes by endocrine cells may aid in the migration of cells to their final locations in the developing gland" (p.601).

1.1.8.4 Role in synaptic plasticity

The expression of neuroserpin alters density and shape of dendritic protrusions, ultimately contributing to synaptic plasticity (Borges, Lee et al. 2010). Tsang, Young et al. (2014) investigated the effects of neuroserpin overexpression in mice through a recombinant adeno-associated virus-mediated gene transfer. Moreover, it was suggested that the neuroserpin functions to regulate synaptic plasticity, although no behavioral changes were observed.

1.1.8.5 Role in the regulation of the emotional state

In experiments conducted with genetically altered mice, these mice exhibited substantial changes in their behavior. Neuroserpin-deficient mice demonstrated an anxiety-like reaction in the O maze test (Fig. 1.7). Both, neuroserpin-deficient and overexpressing mice exhibited neophobic responses in the novel-object test. All animals in the study appeared to be healthy and showed no anatomic or neurologic deficits. These anxiety-like and neophobic responses are amazing, since this is the first evidence of an inhibitory protein causing behavioral changes. The mechanisms involved remain unknown (Madani, Kozlov et al. 2003).
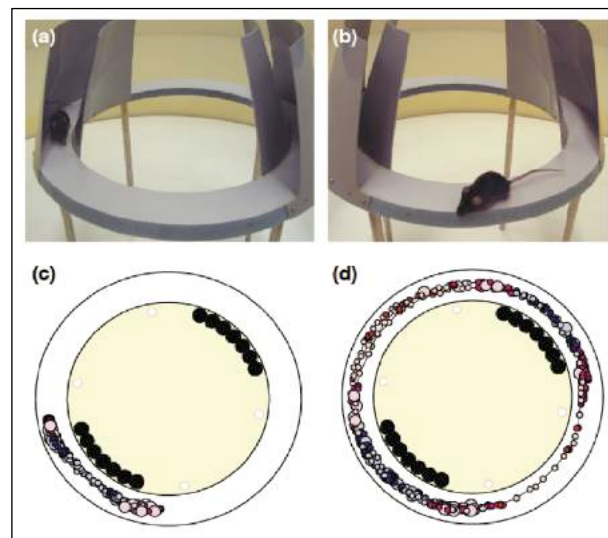
Figure 1.7: O maze experiment displaying altered behavior in neuroserpin-deficient mice. When placed in an elevated-O maze, mutant mice (a) avoid the open sectors, as compared with their wild-type littermates (b). Tracking analysis is illustrated for mutant (c) and wild-type (d) mice.
Image and description adopted from (Madani, Nef et al. 2003).

1.1.8.6 Neuroprotective role

Another feature with possibly clinical applications is the neuroprotective character of neuroserpin. Not only in transgenic mice, but also when administrated, neuroserpin reduces infarct volume. Microglial activation is attenuated, leading to reduced postischemic inflammation and therefore less severe neurological outcome (Cinelli, Madani et al. 2001; Zhang, Zhang et al. 2002; Gelderblom, Neumann et al. 2013).

Also studied is the early ischemic preconditioning by neuroserpin in cortical and hippocampal neurons (Wu, Echeverry et al. 2010). During sublethal ischemic injury, expression of neuroserpin is increased in the hippocampus and in all cortical layers. Neuroserpin is thought to inhibit excitotoxin-induced cell death, hence increasing neuronal survival after cerebral ischemia. As a neuroprotective, neuroserpin enhances neuronal survival in seizure and delays seizure progression itself (Yepes, Sandkvist et al. 2002).

1.1.9 Involvement in pathogenesis

1.1.9.1 Alzheimer's disease

In patients with Alzheimer's disease, neuroserpin has been found to co-localize with beta amyloid (Aβ) peptides within amyloid plaques (Kinghorn, Crowther et al. 2006). Since the amyloid precursor protein (APP) gene is located on chromosome 21, patients suffering from Down syndrome are prone to develop Alzheimer's disease. Concordant with this finding is the upregulation of neuroserpin mRNA and protein in brains of Down syndrome patients (Iulita, Do Carmo et al. 2014). Kinghorn, Crowther et al. (2006) demonstrated Aβ to be bound by neuroserpin and a reduction of the oligomer toxicity, whereas Fabbro, Schaller et al. (2011) reported neuroserpin-deficient mice to have reduced Aβ levels and less spatial memory loss. These findings are fairly contradictory and suggest the necessity of future research on this topic.

1.1.9.2 Cancer

For several years, other serin protease inhibitors have been associated with cancers. The discovery of the predictive value of PAI-1 in breast cancer even led to its clinical use as a marker protein (Harbeck, Thomssen et al. 1999).

"Metastases are responsible for the majority of deaths from cancer. Dissemination of primary cancers to secondary organ sites is most ominous when tumors spread to the brain. Brain metastases indicate poor prognosis, likely exclusion from clinical trials, and cause neurologic deficits that impair patient's lives in fundamental ways. Existing therapies are restricted to palliative radiation and neurologic surgery, with limited chemotherapeutic options"
(Termini, Neman et al. 2014, p.4011).

A recent study indicated that brain metastases are protected by neuroserpin. Expression levels of neuroserpin mRNA is elevated in brain metastatic cells from lung and breast cancer types. Along elevated expression levels of neuroserpin vascular co-option by malignant cells is increased and metastatic spread is facilitated. The mechanism involves the plasminogen activator (PA) – plasmin system. Plasmin depletes infiltrating cells via release of the Fas ligand, an apoptosis inducing transmembrane protein from reactive astrocytes. It was suggested that cell death of infiltrating cells occurs, unless soluble Fas levels are decreased by inhibition of PA through neuroserpin. Moreover, the L1 cellular adhesion molecule (L1CAM) was found to mediate metastatic spread. L1CAM is eliminated by plasmin, as well. Metastatic traits benefit from augmented interactions of L1CAM through neuroserpin dependent

inhibition of PA. Combined, neuroserpin shields metastatic cells from death signals and fosters their outgrowth in the brain (Fig. 1.8). This recent discovery of neuroserpin as a pro-metastatic protein possibly bears potential for biologic therapy of brain cancers (Valiente, Obenauf et al. 2014).
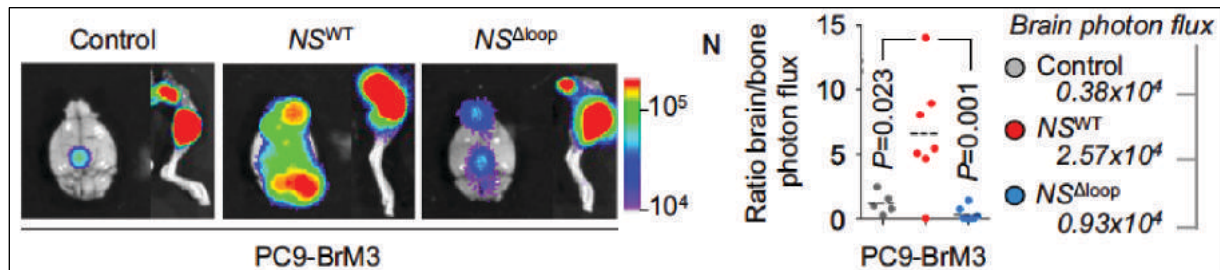
Figure 1.8: Illustration of the prometastatic qualities of neuroserpin.
Ex vivo bioluminescence images of brains and hindlimbs 21 days after inoculation with PC9-BrM3, a metastatic tumor cell line, in mice (A). Vectors applied were an empty vector (Control), a vector encoding wild-type neuroserpin (NS^{WT}) or reactive center loop mutant neuroserpin ($NS^{\Delta loop}$) that is deprived of PA inhibitory function. Wild-type neuroserpin markedly increases metastatic activity in the brain, whereas the mutant does not.
Ratio of photon flux in brain versus bone of hindlimb and brain photon flux mean values demonstrate the prometastatic activity of neuroserpin being confined to the brain (B). While PC9-BrM3 is also metastatic to bone, neuroserpin overexpression did not result in increase of bone metastases.
Images and descriptions adopted and modified from (Valiente, Obenauf et al. 2014).

1.1.9.3 Schizophrenia

Beyond the forementioned pathogenic qualities, there are more diseases associated with the SERPINI1 gene. For instance, it is hypothesized that schizophrenia may be a neurodevelopmental disease (Raedler, Knable et al. 1998; Hakak, Walker et al. 2001). However, schizophrenia has a high genetic component (Sullivan, Kendler et al. 2003). DNA microarray analysis in postmortem cortex samples of schizophrenic patients revealed up-regulation of the neuroserpin gene (Hakak, Walker et al. 2001). In a recent study, human induced pluripotent stem cell (hiPSC) neurons were produced from patients suffering from schizophrenia. When compared to a control group, the hiPSCs from schizophrenic patients had diminished neuronal connectivity and decreased neurite numbers. Subsequent microarray studies of the schizophrenic hiPSCs revealed 5-fold upregulation of SERPINI1 along many other deregulated genes (Brennand, Simone et al. 2011).

1.1.9.4 FENIB

The leading cause of pathologies associated with neuroserpin is the accumulation of neuroserpin polymers in familial encephalopathy with neuroserpin inclusion bodies (FENIB). FENIB is a conformational disease, characterized by an aggregation of aberrant proteins.

Belonging to the family of serpinopathies, this disease is caused by a "toxic gain of function" from the accumulated protein (Irving, Ekeowa et al. 2011).

Aberrant neuroserpin proteins are caused by point mutations in regions that are critical for conformational stability. The resulting instability causes the protein to fold into an intermediate conformer, which is susceptible to polymerization. Another native neuroserpin is added to the monomeric intermediate conformer. After formation of a dimer, aggregation advances either by monomer or polymer addition (Noto, Santangelo et al. 2012). Mutant neuroserpin is glycosylated, but not secreted (Yazaki, Liepnieks et al. 2001; Galliciotti and Sonderegger 2006). It is also noteworthy that wild-type neuroserpin will also form polymers under near physiologic conditions (Sarkar, Zhou et al. 2011).

Polymers accumulate within the membranes of the rough endoplasmatic reticulum. These accumulations, called Collins bodies (Fig. 1.9), can be stained with periodic acid-Schiff (PAS) and are diastase resistant. Collins bodies have been found in the gray matter of the cerebral cortex, especially in deeper cortical layers, subcortical nuclei, spinal cord, and in dorsal root ganglion cells (Galliciotti and Sonderegger 2006).
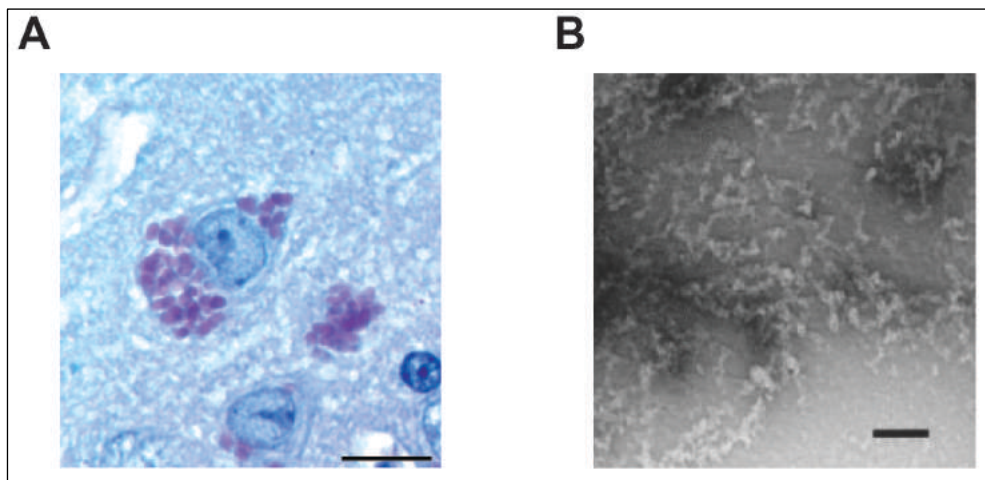
Fig. 1.9: Collins bodies revealed by PAS staining of brain sections of a Portland mouse aged 6 months identical to those observed in FENIB patients (A). Electron microscopy of intact Collins bodies found in a FENIB patient (B). Scale bar (A)=100 μm, (B)=100nm.
Image (A), including description, adopted and modified from (Galliciotti, Glatzel et al. 2007).
Image (B), including description, adopted and modified from (Davis, Shrimpton et al. 1999).

FENIB first has been described in two Caucasian families in the USA. Their symptoms ranged from cognitive decline to progressive dementia, seizures, and myoclonus (Davis, Shrimpton et al. 1999). Point mutations were discovered that led to the amino acid substitutions Ser49Pro (PI12$_{Syracuse}$) in one family and Ser52Arg (PI12$_{Portland}$) in the other

family. Both mutations are inherited autosomal dominantly (Galliciotti and Sonderegger 2006).

Recently, six mutations leading to clinical symptoms have been described: Leu47Pro, Ser49Pro, Ser52Arg, His338Arg, Gly392Glu, Gly392Arg (Belorgey, Irving et al. 2011; Hagen, Murrell et al. 2011). Each mutation variant results in a certain degree of instability, ultimately prompting a certain rate of polymerization, intracellular accumulation, age of onset and severity of symptoms in a direct relationship (Galliciotti and Sonderegger 2006; Irving, Ekeowa et al. 2011). For example, the patient with the mutation Gly392Glu developed progressive myoclonus epilepsy two years earlier than the patient with His338Arg. Her cause of death was due to status epilepticus at the age of 19 (Galliciotti and Sonderegger 2006).

Despite the fact that polymers are produced throughout life, the disease mainly affects the adult patient. Studies suggest that polymers are degraded by the endoplasmatic-reticulum-associated protein degradation system (Schipanski, Oberhauser et al. 2014). Since minimal accumulations remain subclinical, the prevalence of FENIB could be higher than originally thought (Galliciotti, Glatzel et al. 2007).

1.2 Tissue Plasminogen Activator

1.2.1 General aspects

Tissue-type plasminogen activator (tPA) is a chymotrypsin-like serine protease. It was first reported under the name fibrinokinase in 1947 (Collen and Lijnen 2009). As a chymotrypsin-like protease, tPA is translated with a N-terminal extension. During processing, the extension undergoes proteolytic cleavage and is removed (Hedstrom 2002).

The processed protease exists as a single-chain (Fig. 1.10) and as a two-chain molecule. The complete single-chain molecule consists of 527 residues (Bode and Renatus 1997) and has a molecular weight of 66kDa (Orth, Madison et al. 1992). Upon cleavage of a peptide bond, the single-chain protein is converted into the proteolytically active two-chain form. Single-chain tPA is unique as it offers some proteolytic activity (10-20% of the two-chain form) (Bode and Renatus 1997).
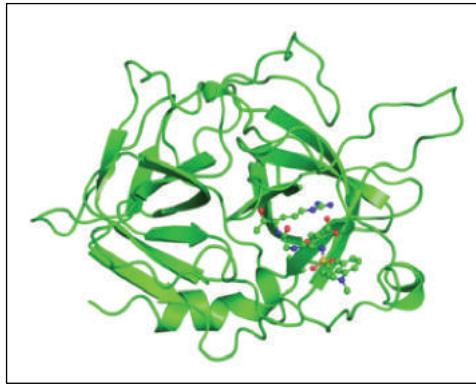
Figure 1.10: 3D crystal structure of human single chain tPA in complex with dansyl-EGR-CMK at 3.35A resolution illustrating monomeric assembly.
Image according to (Renatus, Engh et al. 1997); adopted from (http://www.ebi.ac.uk/pdbe-srv/view/entry/1bda/summary) on 09-02-14, 5:30pm UTC+1.

tPA is expressed in endothelial cells of the vascular system, neurons of the CNS and PNS, microglial cells, astrocytes, and in the mesothelial cells of the peritoneum (Kruithof and Dunoyer-Geindre 2014). Intracellularly, tPA localizes to Weibel-Palade bodies in endothelial cells and generally to small storage granules (Rosnoblet, Vischer et al. 1999; Knipe, Meli et al. 2010). Secretion is triggered by an increase of Ca^{2+} or via cAMP (Tranquille and Emeis 1991; Tranquille and Emeis 1993; Kruithof and Dunoyer-Geindre 2014).

PAI-1 is recognized as the principal inhibitor of tPA. As discussed above, the serine protease inhibitor neuroserpin interacts with tPA, as well as other serpins, including PN-1, plasminogen activator inhibitor-2, and α2-antiplasmin. Clearance of tPA occurs via mannose receptors or LRP (Kruithof and Dunoyer-Geindre 2014).

The main task of tPA is the removal of fibrin clots in the vascular system. Lysis of fibrin is achieved by plasmin. Prior, the inactive plasminogen has to be cleaved by tPA in order to be activated. Without binding to fibrin, tPA only insufficiently catalyzes the activation of plasminogen to plasmin. The binding process of tPA and plasminogen to fibrin was revealed to occur in a sequential fashion, resulting in a cyclic ternary complex. In the cyclic complex, tPA has a much higher affinity to its substrate plasminogen (Hoylaerts, Rijken et al. 1982; Collen and Lijnen 2009).

Besides fibrin of the fibrinolysis pathway, there are many other proteins, such as annexin II, beta2-glycoprotein 1, voltage-dependant anion channels, Aβ, and denatured proteins which enhance tPA activity by binding to tPA and plasminogen (Kruithof and Dunoyer-Geindre 2014). tPA has a short half-life of six minutes in humans, mainly due to rapid hepatic clearance (Collen and Lijnen 2009). The short duration of action and the availability of the antagonist aminocaproic acid make it a valuable fibrinolytic agent in clinical settings. In 1983, purified tPA from a melanoma cell line was successfully applied in acute myocardial

infarction patients for the first time (Collen and Lijnen 2009). Today, the recombinant tPA (r-tPA) usually is administered in embolic stroke, myocardial infarction and pulmonary embolism. The translational process from generation of r-tPA to clinical application is considered as "one of the fastest drug development projects in history" (Collen and Lijnen 2009, p.1154).

In the nervous system, tPA is thought to assume many roles. Contained in vesicles, tPA is not secreted via constitutive pathway, but rather released upon membrane depolarization or stimulus. It is involved in synaptic plasticity, memory, and emotional and motor learning through several mechanisms (Melchor and Strickland 2005).

tPA-induced activation of matrix-metalloproteinase-9 (MMP-9) is suggested to facilitate neurogenesis and axonal regeneration. Furthermore, the fibrinolytic activity of tPA protects against axonal degeneration and demyelination (Akassoglou, Kombrinck et al. 2000). On the other hand, interaction with LRP also enables tPA to pass the blood brain barrier without affecting its integrity (Benchenane, Berezowski et al. 2005). Therefore, interaction with MMP-9 can lead to disruption of the blood brain barrier, exposing the CNS to higher damage in conditions like multiple sclerosis (Benarroch 2007).

1.2.2 Pathological aspects

1.2.2.1 Addiction

Substance addiction can be considered a pathological consequence of synaptic plasticity. tPA expression is increased in the limbic system, the nucleus accumbens and in astrocytes of the spinal cord in models of alcohol or morphine addiction (Melchor and Strickland 2005; Berta, Liu et al. 2013). tPA- and plasminogen-deficient mice were demonstrated to exhibit less addiction related behavior when treated with morphine (Nagai, Yamada et al. 2004). Contrary, tPA induces morphine tolerance, a classic symptom of addiction, and development of pain hypersensitivity (Berta, Liu et al. 2013). Morphine and Nicotine induce tPA-regulated dopamine release (Nagai, Yamada et al. 2004; Nagai and Yamada 2008). In chronic ethanol abuse, tPA upregulates the number of NMDA receptors responsible for seizures in ethanol withdrawal (Pawlak, Melchor et al. 2005).

1.2.2.2 Alzheimer's disease

In Alzheimer's disease, the tPA-plasmin axis has been implicated in the breakdown of Aβ. On a molecular level, tPA binds to the fibril sides of amyloid (Beringer, Fischer et al. 2013).

Diminished levels of the fibrinolytics cause the occurrence of a vicious cycle where high amounts of amyloid upregulate PAI-1 activity, in turn inhibiting tPA (Melchor and Strickland 2005).

1.2.2.3 Stroke

The role of tPA in inflammation and stroke has been thoroughly described. In general, neurovascular damage is potentiated by tPA in any kind of trauma to brain parenchyma. Post-traumatic inflammation is mediated by tPA by excessive microglia activation (Gelderblom, Neumann et al. 2013). High vascular permeability associated with the inflammation gives rise to brain edema (Yepes, Sandkvist et al. 2000), a feared complication with high morbidity and death (Raslan and Bhardwaj 2007). High concentrations of tPA directly translate into enlarged infarct size, whereas low concentrations inflict less injury (Nagai, De Mol et al. 1999). Hence, regulation of tPA is suggested to be "beneficial in controlling infarct injury after stroke" (Melchor and Strickland 2005, p.5).

1.3 Proprotein convertases

The family of proprotein convertases (PCs) comprises nine different secretory mammalian serine proteases (Fig. 1.11). This set of enzymes was discovered through the identification of their related yeast convertase kexin. As a consequence, any member of the family is also termed as proprotein convertase subtilisin/kexin type 1 to 9 (Pcsk1 to Pcsk9). A shared characteristic of the first seven PCs is the cleavage of proproteins trafficking through the secretory pathway that is performed at single or pairs of basic residues. Pcsk8 cleaves at non-basic residues, while Pcsk9 cleaves itself for its activation (Seidah 2011).
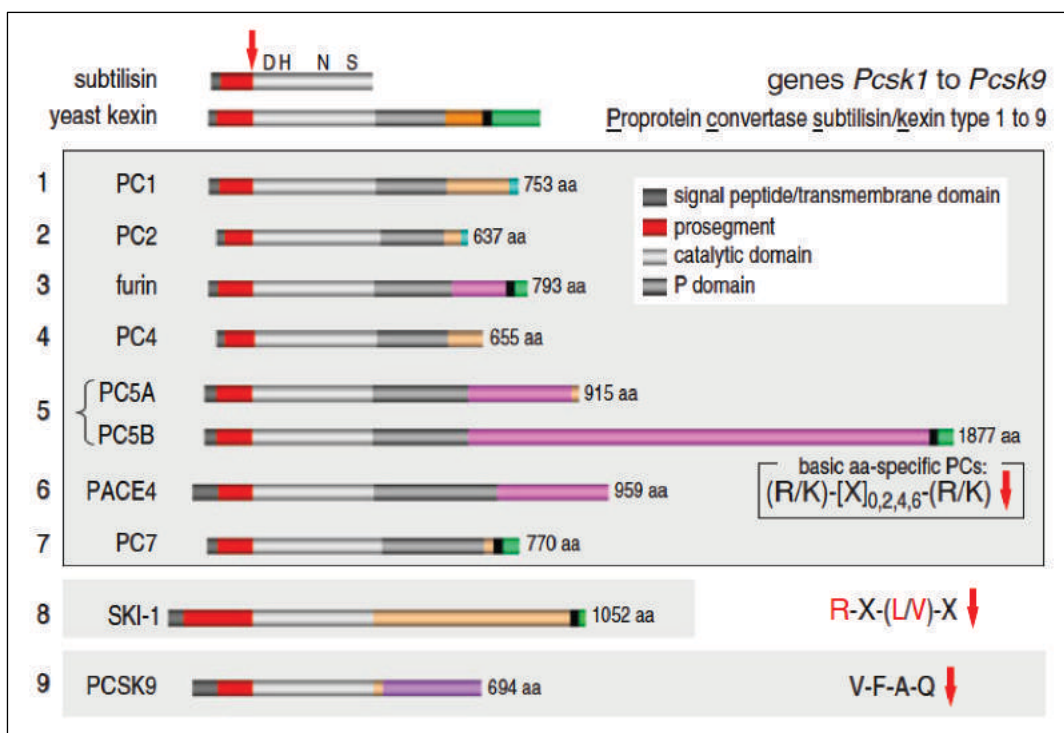
Figure 1.11: Schematic primary structures of the nine PCs. Bacterial subtilisin and yeast kexin are also included. Red arrow indicates cleavage site. Specifically recognized motifs are shown with their accordingly boxed convertases. X = variable amino acid.
Image adopted from (Seidah 2011), description according to (Seidah 2011).

1.3.1 PC1/3

PC1/3 is a crucial enzyme in processing of prohormones and proneuropeptides. During maturation, the inactive proPC1/3 undergoes several activation steps, including autocatalytical cleavage of the N-terminal prosegment in the ER and *trans*-Golgi-network (TGN). At the TGN, it already may act on its substrates. Finally, it is directed into secretory granules and truncated C-terminally. Therefore, PC1/3 controls the regulated secretory pathway at several

locations, including within secretory granules in the mature form. The active murine proteins weigh 87kDa and 66kDa (C-terminal cleaved) (Benjannet, Rondeau et al. 1993; Seidah 2011; Seidah, Sadr et al. 2013).

Concerning the distribution in the body, PC1/3 is exclusively found in endocrine cells. Within the pituitary, it is concentrated in the anterior lobe and its expression increases fom E15 to adulthood (Marcinkiewicz, Day et al. 1993).

Although not indispensable for life, PC1/3-null mice revealed pre-/perinatal lethality, as well as developmental defects like achondroplasia and intellectual disabilities. In humans, few patients with Pcsk1 deficiency have been reported. Symptoms involved glucose homeostasis, obesity and infertility due to misprocessing of POMC and proinsulin. In addition, absorption defects of the small intestine were causing massive diarrhea. Ghrelin is an appetite-inducing hormone and affiliated with hyperphagia in pathology. The processing of proghrelin to ghrelin requires PC1/3. This can be one of the causes of early-onset obesity found in PC1/3-deficient patients (Seidah 2011; Seidah, Sadr et al. 2013). Likewise, overexpression of PC1/3 recently was suggested to contribute to pathogenesis of nasal polyps (Lee, Lee et al. 2013).

1.3.2 PC2

PC2 plays a crucial role in the processing of neural or endocrine peptides and in generating morphinomimetic peptides. Together with PC1/3, the two PCs often have same substrates and are considered the "ying and yang of body mass and energy homeostasis, with PC1/3 playing a restraining role and PC2 playing a promoting one" (Seidah, Sadr et al. 2013, p.21475). Unlike PC1/3, PC2 is kept inactive during trafficking. The inhibition is provided by its chaperone 7B2 which safeguards proper folding. Activation of PC2 only occurs within secretory granules, yielding the mature form of 68kDa. Together with PC1/3 it is found in endocrine cells which are contained in the brain pituitary, but also other organs such as the small intestine (Gagnon, Mayne et al. 2009).

Although PC1/3 and PC2 perform many catalytic processes together in an orchestrated manner, PC2 has its own unique characteristics. Contrary to PC1/3, it is more concentrated in the intermediate lobe of the pituitary. In the developing brain, PC2 generally is more widely distributed than PC1 (Zheng, Streck et al. 1994). Likewise, only PC2, but not PC1/3 is produced in invertebrates like *Drosophila melanogaster*. PC2-null mice exhibit growth

retardation, glucose tolerance and obesity resistance. However, the number of pups born was not decreased (Benjannet, Rondeau et al. 1993; Seidah, Sadr et al. 2013).

Many neuropeptides involved in nociception (e.g., endorphins or nociceptin, etc.) are considered potential substrates for PC1/3 and PC2. PC2-deficient mice exhibited enhanced stress-induced analgesia, supposedly due to either accumulation of opioid precursors or loss of anti-opioid peptides (Croissandeau, Wahnon et al. 2006).

The processing of the pro-opiomelanocortin (POMC) by both PCs is of particular interest for this work. POMC is a 241 amino acid prohormone mainly produced amongst different locations in the pituitary gland. The fact that it is also expressed in tissues other than the pituitary, such as the skin and the arcuate nucleus or the cortex is a prime example of tissue specific processing. In this concept, a varying range of secretory products can be created upon specific cleavages from the identical precursor, depending on the processing enzymes present in each tissue (Fig. 1.12). In the anterior lobe of the pituitary, the predominant PC1/3 is responsible for conversion of POMC into adrenocorticotropic hormone (ACTH) and β-lipotropic hormone (β-LPH). In the intermediate lobe, PC2 additionally cleaves PC1/3 cleavage-derived peptides into α-melanocyte-stimulating hormone (α-MSH) and β-endorphin (Bicknell 2008).

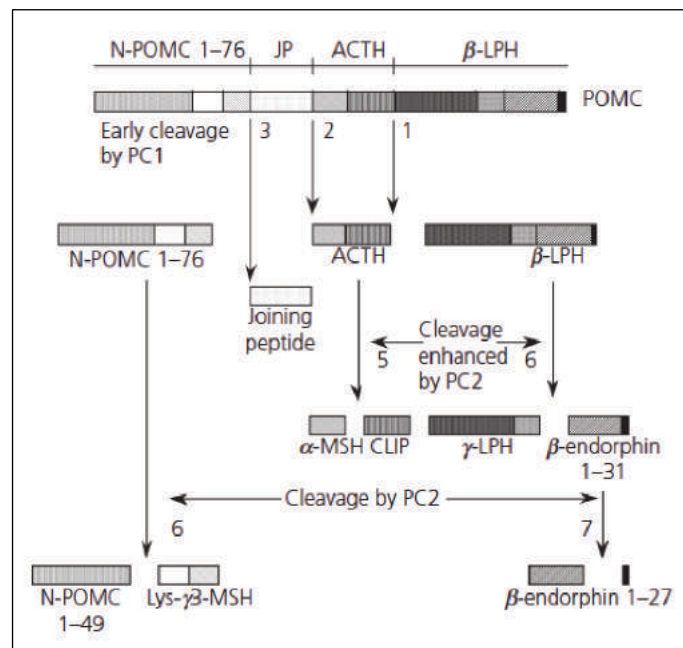*Figure 1.12: Processing of pro-opiomelanocortin (POMC) by prohormone convertases 1 and 2. The dibasic sites are cleaved in the specific order illustrated by the numbers, showing that PC2 acts on the products of PC1/3 cleavage. ACTH, adrenocorticotropin; CLIP, corticotrophin-like intermediate peptide; LPH, lipotrophin; MSH, melanocyte-stimulating hormone.*
Image and description adopted from (Bicknell 2008).

The resulting products are of central function in the human body. ACTH is a hormone that stimulates release of corticosteroids from the adrenal gland. The melanocyte stimulating α-MSH induces dark coloring of skin and hair. Next to phenotypic changes, it also has an impact on the brain as it induces appetite or sexual arousal (Hughes, Everitt et al. 1988). Hence, important physiologic functions are indirectly controlled by PC1/3 and PC2. Although, processing of POMC can take place in many tissues, general consensus is that "the vast majority of POMC peptides found in the circulation are derived from the pituitary whereas, by contrast, peptides produced in extra-pituitary tissues act in an autocrine or paracrine fashion" (Bicknell 2008, p.694).

Similarly to regulation of POMC, the PC couple cleaves several other peptides. These peptides include proinsulin, enkephalins and/or chromogranins as they play a central role in homeostasis and pathologic conditions. Despite the differences in processing, both PCs are directed to and reside in secretory granules. Their catalytic activity is Ca^{2+} dependent. Although, separately not essential for life, lack of both enzymes causes death during embryogenesis (Seidah 2011). Due to their involvement in several physiologic pathways, alterations of their concentrations are frequently found in disease. Concentrations and activity of PC1/3 and PC2 are altered in liver colorectal metastasis (Tzimas, Chevet et al. 2005). In Huntington disease patients, expression was reduced in specific brain regions (van Wamelen, Aziz et al. 2013). Regardless of the expression patterns of PC1/3 and PC2, their role in these pathologies yet remains to be explained.

1.3.3 Furin

Furin is a 794 amino acid type-1 transmembrane protein. It is ubiquitously expressed in mammals. Initially named FUR due its gene laying upstream of the oncogene FES encoding region, it is also known as PACE (paired basic amino acid cleaving enzyme) (Kiefer, Tucker et al. 1991; Thomas 2002).

The translated protein contains a prodomain which serves two purposes. One is to safeguard proper folding as an intramolecular chaperone. The other is to keep the protein inactive before maturation. Furin performs autoactivation by cutting its own prodomain twice. The first cut occurs ($t_{1/2}$ = 10min) in the ER. The second cleavage of the prodomain ($t_{1/2}$ = <2h) happens in the TGN/endosomal system. Due to the particular pH of each compartment, each autoactivational step can only occur at its destined site. Intracellularly, Furin localizes to the TGN by its bipartite motif. This motif is necessary for sorting from TGN to endosomes and

retrieval from endosomes back to TGN. At this point, trafficking of Furin is carried out in the regulated as well as in the constitutive pathway. Starting from the TGN, the budded proteinase is sent to the plasma membrane in the constitutive/basolateral pathway. In the regulated pathway, budded Furin is conveyed to and stored in secretory granules. The granules are released upon proper stimuli. Endocytosis resembles another way for a cell to gather the proprotein convertase. If the Furin protein happens to appear near the cell surface, it may be tethered to it by filamin molecules. After endocytosis, Furin is redirected to the TGN within endosomes, which also enables its recycling to the cell surface (Thomas 2002). Its transmembrane domain fixes Furin to the cell membrane. In a postranslational process called "shedding", Furin undergoes C-terminal truncation between Ser^{682} and Arg^{683} (Plaimauer, Mohr et al. 2001). The naturally secreted "shed Furin", now lacking its transmembrane domain and cytosolic tail, is a fully functional enzyme and was detected *in vivo* in epididymal fluids of mammals where it is thought to pursue particular tasks (Thimon, Belghazi et al. 2006).

Furin processes a wide array of proteins, including metallo-proteinases, growth factors, hormones, cell surface receptors and plasma proteins (Mayer, Boileau et al. 2004). Due to its abundant localization and pathways from TGN to plasma membrane and back during trafficking it is considered a housekeeping enzyme. As a result, Furin plays a crucial role in embryogenesis. Transcription of the Furin gene is upregulated as early as in human trophoblast syncytialization (Zhou, Wang et al. 2014). Lack of Furin in knock-out mice results in prenatal death around E11 due to impaired axial rotation and associated dysgenesis of the heart (Roebroek, Umans et al. 1998).

Specifically in the CNS, Furin processes growth factors and adhesion molecules (Seidah 2011). Pro-β-nerve growth factor (pro-β-NGF), the pro-form of the neurotrophin NGF is cleaved by Furin. The yielded NGF mediates synaptic innervation. However, if processing of pro-β-NGF is diminished, increased secretion of the pro-form will induce apoptosis (Lee, Kermani et al. 2001). Moreover, Furin-mediated processing of repulsive guidance molecule (RGMa) directs axonal growth (Tassew, Charish et al. 2012). According to Thomas (2002), these findings suggest that Furin activity might regulate the neural network architecture. This universal enzyme is involved in neuropathologic conditions. Furin mRNA has been described to accumulate in immature senile plaques (Marcinkiewicz 2002) and decreased levels of Furin are suggested to cause Aβ production in Alzheimer's disease (Hwang, Kim et al. 2006). In

primary brain cancer, the enzymatic activity of Furin is protective (Maret, Sadr et al. 2012). Yet, inhibition of Furin shields from tumor growth in various other malignancies, making its role in cancer to seem somewhat controversial (Ma, Fan et al. 2014; Scamuffa, Sfaxi et al. 2014).

Furin is ubiquitously expressed and processes many different precursor molecules with its pathogenic involvement not restricted to the CNS. For example, a positive feedback loop with transforming growth factor beta (TGF-β) that is located in synoviocytes promotes ADAMTS-4-dependent breakdown of cartilage aggrecan leading to rheumatoid arthritis. Next to the processing of intrinsic proteins, Furin activates a large number of bacterial toxins. Processed toxins include anthrax toxin, diphtheria toxins, *Pseudomonas* exotoxin A, *Clostridium septicum* α-toxin, shiga toxin and shiga-like toxin-1. This trait finally renders these toxins to the hazardous agents they are and causes Furin activity undesirable in bacterial infection. Moreover, the threat deriving from bacterial toxins is overshadowed by the pathogenic viruses, which utilize Furin. HIV-1, Ebola virus, measles virus, respiratory syncytial virus (RSV) and avian influenza virus are dependent on cleavage by Furin to activate their immature envelope glycoproteins. Interestingly, the degree of consensus cleavage sites specific to Furin directly correlates with the virulence of certain strains (Thomas 2002).

1.4 YFP-PCA

In the course of their studies on the chemiluminescent protein aequorin, Shimomura, Johnson et al. (1962) discovered the green fluorescent protein (GFP) in *Aequoria* jellyfish. Soon they learned that GFP converted blue light deriving from aequorin into green light, thus exhibited excitation and emission peaks of different wavelengths. GFP is a cylindrical shaped protein whose peptide backbone carries a chromophore in the center of the cylinder. The chromophore is a *p*-hydroxybenzylideneimidazolinone, formed by the residues 65-67 of the protein. Cloning of the gene and expression in host organisms proved that the genetic code suffices to reproduce the functional protein, including the chromophore. Having been successfully targeted to every cell compartment, GFP does not seem to inflict any major cytotoxic effects. For this reason, GFP is widely used in natural sciences as a marker of subcellular localization, as a reporter protein of expression or as an indicator of protein-protein interaction (Tsien 1998). For their discovery and development of GFP, Shimomura, Tsien and Chalfie were awarded the Nobel Prize in chemistry in 2008 (Zimmer 2009).
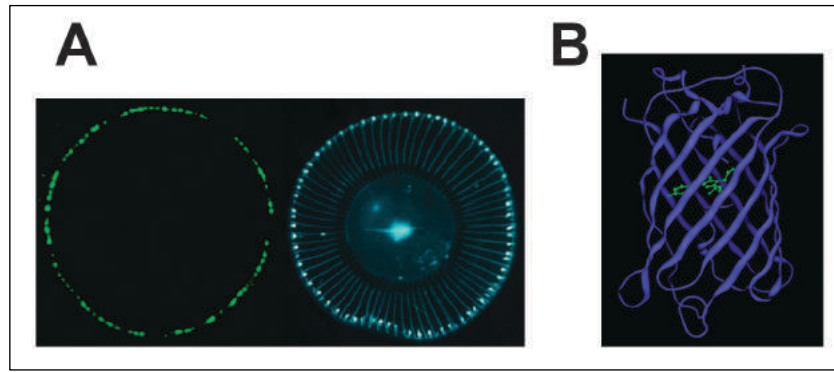
Image 1.13: Aequorea victorea in the dark (left) and under visible light (middle). (A)
Crystal structure of GFP. The chromophore is shown in green and is located in the center of the β-barrel. (B)
Images and description adopted from (Zimmer 2009).

A relatively novel use of GFP is the split-assembly based detection of protein interaction. When exposed to light of a wavelength close to its excitation peak, the fluorescent protein emits light of a different wavelength. Thus, a functional fluorescent protein is able to yield observable light when excited. In addition, the protein can be split in two N- and C-terminal halves. These halves are not able to deliver fluorescence. If brought into a sufficient vicinity, the halves spontaneously fuse to a fully functional fluorescent protein again. This property is used in the protein complementation assay (PCA), where fluorescent protein fragments are tagged to "bait" and "prey" proteins. In case of interaction between the two proteins investigated, the tagged reporter protein fragments are able to fuse. The interaction now is detectable in fluorescence microscopy (Wilson, Magliery et al. 2004; Taraska and Zagotta 2010).
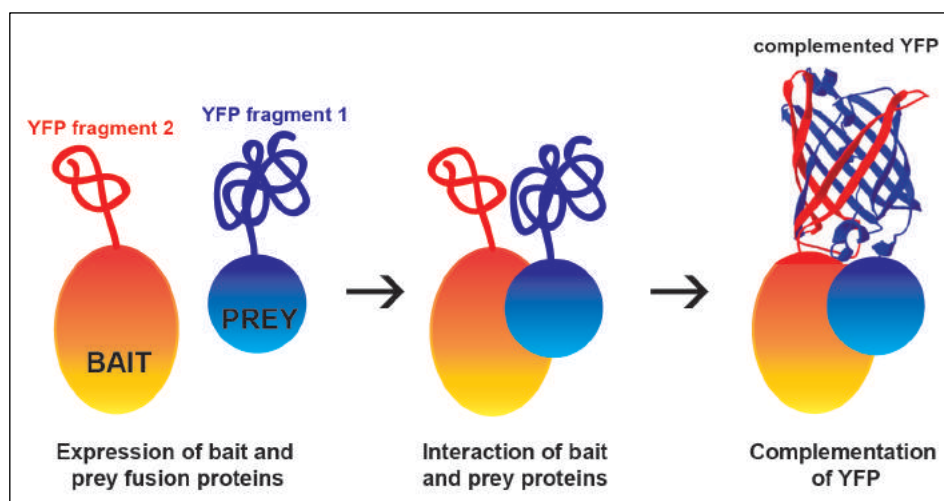

Figure 1.14: sketch of YFP-PCA clarifying the complexation-induced fusion of split fragments, which are fused to the bait/prey investigated.
Image adopted and modified according to (Nyfeler, Reiterer et al. 2008).

In 2005, Nyfeler, Michnick et al. studied the protein interactions in the secretory pathway by applying this approach using the yellow fluorescent protein (YFP). This protein is a genetic mutant of GFP with slightly altered excitation and emission peaks. Their engineered constructs served as blueprint for this work. An advantage of the YFP-PCA is that weak interactions are stabilized by the complementation of the tags. In addition, any interaction can be detected *in vivo* at the site where it takes place, such as the dense-cored granules of the secretory pathway. These characteristics are especially interesting to us, since the proteins we presume as putative targets are conveyed through different pathways. Furthermore, complexes with neuroserpin exhibit a short half-life and protease activity of reported *in vivo* complexes with neuroserpin is unaffected. Therefore, we intend to reveal any protein-protein interaction with YFP-PCA that otherwise would not be observed by conventional methods.

2 Material and Methods

2.1 YFP-tag constructs

Subcloning of YFP fragments into pcDNA3.1 vectors has been described previously by Remy, Montmarquette et al. (2004); whereas, Nyfeler, Michnick et al. (2005) studied the comprising sequences of YFP1 (amino acids 1-158) and YFP2 (amino acids 159-239). Neuroserpin is known to be cleaved at its C-terminal end in complex formation (Ricagno, Caccia et al. 2009). To avoid loss of the tags during complexation, each split YFP fragment was fused via a four amino acid long linker to the N-terminal end of either wild type or mutant murine neuroserpin. In proteases (tPA, PC1/3, PC2, Furin, trFu), tags were linked C-terminally, due to cleaving of the prodomain at the N-terminus (Benjannet, Rondeau et al. 1993; Hedstrom 2002; Thomas 2002). Positive control for transfections was human neuroserpin linked to a full length Green Fluorescent Protein (GFP) at the C-terminus. The empty pcDNA3.1 vector served as a negative control. All constructs were a gift from Dr. Giovanna Galliciotti (Institute of Neuropathology, University Medical Center Hamburg-Eppendorf) with the exception of the positive controls for complementation assay (GCDH1, GCDH2), which were a gift from Dr. Jessica Lamp (Children's Hospital, Department of Biochemistry, University Medical Center Hamburg-Eppendorf).

2.2 Subcloning of POMC cDNA

For later use in transfections POMC cDNA (Source BioScience LifeSciences, Nottingham, UK) was subcloned from pDNR-LIB into a pcDNA3.1 vector. The cDNA was digested with "EcoR1" and "HindIII". 6μg POMC cDNA in pDNR-LIB or 2,5μg pcDNA3.1 were mixed with 5μl 10x FastDigest buffer (Fermentas/Thermo Fisher Scientific, Waltham, USA), 2,5μl EcoR1 restriction enzyme, 2,5μl HindIII restriction enzyme, filled up to 50μl total with dist. H_2O, vortexed and kept at 37°C for 1h. To check the quality of the restricted vector and DNA, an agarose gel electrophoresis was performed. Digested POMC cDNA shows at approx. 700bp, digested pcDNA at approx. 5400bp. The proper bands were excised from a 1% agarose gel for purification. Insert DNA and destination vector were purified with the GeneJET Gel Extraction Kit (Fermentas/Thermo Fisher Scientific, Waltham, USA) according to the guidelines of the manufacturer. For Ligation, 100μg of resulting vector and 40μg of

resulting insert were mixed with 1µl 10x FastDigest buffer and 0,6µl Ligase to yield a total of 10µl. As a vector control dist. H_2O was added instead of adding the insert. Ligated DNA and vector control each were transformed into XL-10-Gold Ultracompetent Cells (Agilent Technologies, Santa Clara, USA) according to the instructions of the manufacturer. Bacteria were plated and cultured on Ampicillin agar plates overnight at 37°C. In vector control cultures no colonies grew. Single colonies of POMC in pcDNA3.1 were picked, dispersed into HSG medium (13,5g tryptone, 12,5g NaCl, 7,0g yeast extract, 17,0g 87% glycerol, 2,3g K_2HPO_4, 1,5g KH_2PO_4, 0,25g $MgSO_4$ x 7 H_2O) containing Ampicillin (1:1000) and incubated overnight under agitation at 37°C. DNA was purified using Mini-Prep (Quiagen, Venlo, Netherlands), quantified by absorbance measurement and given to sequencing.

2.3 Cell culture and DNA transfection

HEK and N2A cells were grown in DMEM, supplemented with 10% FBS. PC12 cells were grown in DMEM, supplemented with 5% FCS and 10% HS.

For Western Blot analysis approx. $6x10^5$ cells per well were plated in 6 well plates (Nunc, Roskilde, Denmark) and incubated overnight. After overnight incubation, cells were transfected by using Lipofectamine 2000 (Life technologies, Carlsbad, USA) with 4µg DNA and 16µl Lipofectamine pro well, followed by change of medium after 3h.

For fluorescence microscopy and FACS sorting, approx. $5x10^4$ cells (HEK, N2A cells) or approx. $2x10^5$ cells (PC12 cells) per well were plated on poly-L-lysine-coated (20µg/ml in borate buffer) cover slips (Deckgläser, rund 12mm, A. Hartenstein, Germany) in 24 well plates (Tissue Culture Testplate, SPL Life Sciences). Transfection was performed as described above after overnight incubation.

2.4 FACS sorting

PC12 cells were transfected in 12 well plate. After overnight incubation, the cells were trypsinized, washed twice in PBS, filtered and transferred in PBS. FACS sorting was performed using a FACSAria III cell sorter (BD Biosciences, San Jose, USA).

2.5 Fluorescence Microscopy

24h after transfection, cells were washed in PBS, fixed in 3.5% paraformaldehyde for 15min and washed again in PBS.

For YFP-PCA, cells were placed in the dark for 3h at room temperature before fixation. Cover slips were mounted on glass slides using Fluoromount (Fluoromount-G, Southern Biotech, Birmingham, USA) and dried overnight at room temperature.

For immunofluorescence, cells were blocked for 1h in PBS containing 10% FCS and 0,1% glycine and incubated for 1h with the primary antibody (mouse-anti-GFP, 1:500, Living Colors, Takara Bio Europe/Clontech, Saint-Germain-en-Laye, France) in PBS containing 1% FCS, 0,1% glycine, 0,1% saponin. Cells were subsequently washed three times in PBS and stained with Alexa Fluor 555 donkey-anti-mouse IgG (1:500, Molecular Probes, Invitrogen, Carlsbad, USA) for 1h. After three final washes in PBS, slides were mounted as described above.

All slides were analyzed by using confocal microscopy (SP5, Leica Microsystems, Wetzlar, Germany). When a set of slides was analyzed, the settings of the microscope (e.g., gain, etc.) were adjusted to the positive and negative control slides of a set. These settings were not subject to change during the analysis of the remaining slides of the set. Image output was defined within the green color range.

Images were cropped and brightness and contrast were adjusted using the ImageJ software (1.46r version, Wayne Rasband, National Institutes of Health, USA).

2.6 SDS-PAGE

Supernatant was taken and centrifuged (10 min/4°C/16,1rcf). Cells were washed with PBS, lysed in 50μl lysis buffer [150mM NaCl, 20mM Tris (pH7,5), 1% Triton X-100, H_20] in the presence of inhibitors (complete Mini EDTA-free, Roche Diagnostics GmbH, Mannheim, Germany), collected, vortexed and put on ice for 10min. After centrifugation of the lysed cells (10min/4°C/16,1rcf) the cell extract was collected. Both, supernatant and cell extract, were separately boiled with loading dye (10x CVL buffer: 10% SDS, 5ml 250mM Tris-HCl pH7,4, 3,5M ß-Mercaptoethanol, 15% Sucrose and Bromphenolblue) at 95°C for 5min and then cooled on ice for 2min. Samples and ladder (PageRuler Prestained Protein Ladder, Thermo Scientific, Rockford, USA) were separated on 10% polyacrylamide gels at 20mA for approx. 2h.

Upper gel	3,1ml dist. H_2O, 1,25ml 4x Upper Tris buffer, 15μl 10% APS, 10μl TEMED, 0,675ml 30% Protogel
Bottom gel	4,1ml dist. H_2O, 2,5ml 4x Lower Tris buffer, 100μl 10% APS, 4μl TEMED, 3,3ml 30% Protogel

Table 1: ingredients of polyacrylamide gels

Running buffer consisted of 250mM TrisBase, 1,92M Glycin and 0,1% SDS. In a similar manner, samples of POMC triple transfections were separated on 15% polyacrylamide gels. Gels were electroblotted onto nitrocellulose membranes (0,2μm, BioRad, Germany) using the Mini Trans-Blot System (Bio-Rad, Hercules, USA) at approx. 60V for 70min. 10x blotting buffer (250mM TrisBase, 1,92M Glycin, add HCl to adjust pH8,3) was diluted to 1x and Methanol was added to 20%. Blots were stained in Ponceau S. After blocking in TBS-T wash [95% TBS-T (10mM tris pH8,0, 150mM NaCl or 5% Polysorbate 20), 5% instant milk] the membranes were probed with primary antibodies overnight at 4°C under agitation and washed 3x5min with TBS-T. Following 1h of incubation with anti-host horseradish peroxidase coupled antibodies (Promega, Madison, USA) under agitation, membranes were washed with TBS-T 3x5min. Signals were visualized by enhanced chemiluminescence, using the SuperSignal West Pico Chemiluminescent Substrate (Thermo Scientific, Rockford, USA).

In SDS-PAGE of the cell extract after FACS, the more sensitive SuperSignal West Femto Chemiluminescent Substrate (Thermo Scientific, Rockford, USA) was used. To compensate for a too strong signal, one positive control was diluted 10x in dist. H_2O.

To expose blots to another antibody, they were submersed into dist. H_2O for 5min at room temperature, stripped in 0,2M NaOH for 5min and transferred into dist. H_2O for 5min again. After blocking in TBS-T wash for 1h at room temperature, blots were probed with primary antibodies overnight at 4°C under agitation and washed 3x5min with TBS-T. Further visualization as described above.

Signal detection and image processing were performed by the Quantity One Software (Bio-Rad, Hercules, USA) under a Universal Hood II (Bio-Rad, Hercules, USA).

2.7 Animals

All animal procedures were performed in accordance with the institutional guidelines of the animal facility of the University Medical Center Hamburg Eppendorf.

Mice in pituitary experiments were 10 weeks old neuroserpin knock-out mice (KO) (Madani, Kozlov et al. 2003), neuroserpin transgenic mice overexpressing human neuroserpin under the control of the Thy1 promoter (Tg) (Cinelli, Madani et al. 2001), and wild-type littermates from the transgenic line (WT). Brain extracts from P0 neuroserpin knock-out mice (KO) (Madani, Kozlov et al. 2003) and from P0 C57BI6 wild-type mice (WT) were obtained from Dr. Giovanna Galliciotti (Institute of Neuropathology, University Medical Center Hamburg-Eppendorf).

2.8 Pituitary protein extracts

To collect a pituitary, the mouse was killed by cervical dislocation. After dissection of the skin and underlying skull, the cerebrum was lifted out and turned upside down to expose the pituitary. The pituitary was homogenized in 30µl homogenization buffer (150mM NaCl, 20mM Tris pH7,5, complete Mini EDTA-free Roche Diagnostics GmbH, Mannheim, Germany; PhosSTOP Phosphatase Inhibitor, Roche Diagnostics GmbH, Mannheim, Germany) in 1,5ml Eppendorf tubes on ice with a Dounce. Afterwards, 1% of Triton X100 was added, the extracts were mixed and then incubated on ice for 1h. Centrifugation of the tubes took place at 20.000g, 4°C for 30min. Supernatant was collected and their protein concentrations were measured by using a Bradford test (BioRad, Hercules, USA) according to

the guidelines of the manufacturer. For blotting, 90µg of protein were diluted with H_2O to yield 60µl total each, 10x CVL buffer was added and the probes were boiled for 5min, cooled on ice and separated by SDS-PAGE. Further blotting was performed as describe above.

2.9 Brain extracts

Mice were killed by cervical dislocation. Brains were isolated and homogenized in homogenization buffer (see above) with a Dounce. Each tube was supplied with up to 1% of Triton X100 and then incubated on ice for 1h. Centrifugation of the tubes took place at 20.000g, 4°C for 30min. Supernatant was collected and the protein concentrations were measured by using a Bradford test (BioRad, Hercules, USA) according to the guidelines of the manufacturer. For blotting, 100µg of protein were diluted with H_2O to yield 30µl total each, 10x CVL buffer was added and the probes were boiled for 5min, cooled on ice and separated by SDS-PAGE. Further blotting was performed as described above.

2.10 Statistics

Data are reported as mean ±SD. Calculation of p-values was performed using Student's t-test.

2.11 Antibodies

Primary Antibody	Manufacturer	Host Species	Dilution
GFP (Living Colors)	Takara Bio Europe/Clontech, Saint-Germain-en-Laye, France	Mouse	WB: 1:5000 Immunofl.: 1:500
Murine neuroserpin (G64A)	P. Sonderegger	Goat	WB: 1:13
PC2 (ab 3533)	Abcam, Cambridge, UK	Rabbit	WB: 1:500
Furin (MON 148)	LifeSpan Biosciences, Seattle, USA	Mouse	WB: 1:1000
ACTH (ab 74976)	Abcam, Cambridge, UK	Rabbit	WB: 1:1000
Tubulin (E7)	Hybridoma Bank, Iowa, USA	Mouse	WB: 1:1000

Table 2.2: properties of primary antibodies; WB = Western blot, Immunofl. = Immunofluorescence.

Secondary Antibody	Manufacturer	Host Species	Dilution
Anti-mouse HRP	Promega, Madison, USA	Goat	WB: 1:5000
Anti-rabbit HRP	Promega, Madison, USA	Goat	WB: 1:5000
Alexa 555 (anti-mouse)	Molecular Probes, Invitrogen, Carlsbad, USA	Donkey	Immunofl.: 1:500
Anti-goat HRP	Promega, Madison, USA	Donkey	WB: 1:5000

Table 2.3: properties of secondary antibodies; WB = Western blot, Immunofl. = Immunofluorescence.

3 Results

3.1 Testing successful transfection and localization of Neuroserpin and targets by Immunofluorescence

Neuroserpin is a serine protease inhibitor (serpin) of the central and peripheral nervous system (Hastings, Coleman et al. 1997; Schrimpf, Bleiker et al. 1997). It undergoes a Michaelis-like complex formation with its target protease (Dobo and Gettins 2004). As previously described in literature, one of its targets is tPA (Hastings, Coleman et al. 1997; Krueger, Ghisu et al. 1997; Osterwalder, Cinelli et al. 1998).

In this work we tested if PC1/3, PC2 and Furin (three members of the proprotein family) to determine if they binded and were inhibited by neuroserpin. Since complexes of neuroserpin and protease are only stable for a limited amount of time (Barker-Carlson, Lawrence et al. 2002), we tried the YFP-PCA approach in order to detect these short-lived complexes in cells by fluorescence microscopy.

In this protein complementation assay, the coding region of a fluorescent protein tag (e.g., yellow-fluorescent protein) is cut into two pieces. One piece is fused with the coding region of the protease, while the other piece is fused with the coding region of neuroserpin. After transfecting both constructs into cells, the protease and neuroserpin, each containing one half of the split fluorescent protein are produced by cellular machinery. In case of neuroserpin-protease interaction, both pieces of the tag are brought into such vicinity that they spontaneously fuse together and form a functional fluorescent protein. By analyzing the cells by fluorescence microscopy when exposed to light of a certain wavelength, cells containing these fluorescent proteins emit light of a longer wavelength, thus signaling positive neuroserpin-protease interaction. If interaction between neuroserpin and protease does not take place, the fluorescent protein fragments cannot fuse. Therefore, there is no fluorescence observed. This split YFP method is known to detect very weak or transient protein-protein interactions. In addition, the YFP reassembly reaction is irreversible according to its in vitro kinetics (Magliery, Wilson et al. 2005).

For our experiments, every protein was cloned with one half of the YFP, either YFP-1 or -2 respectively. For neuroserpin we tested the wild-type "NS-WT" and as negative control "NS-RM". For this negative control, Proline-Proline were substituted with Arginine-Methionine in the reactive center loop of neuroserpin and also cloned with split-YFP tags.

An empty vector ("pcDNA") served as negative control. Neuroserpin, containing a green fluorescent protein as a whole ("NS-GFP"), served as positive control for successful transfection. "GCDH1+2" consists of a protein that forms homodimers, fused to YFP-1 or YFP-2 tags. These constructs had successfully been used in the past by another research group (Lamp, Keyser et al. 2011). We used these constructs as a positive control specifically for the aspect of the protein complementation assay. Combinations of non-complementary tagged proteins were used as negative controls in double transfections, as well.

At first, we wanted to confirm expression of neuroserpin and its putative targets by using immunofluorescence. We transfected N2A (NS, PC1/3 and PC2) or HEK cells (Furin) with YFP-2-tagged constructs. The YFP-2 split protein can be bound by anti-GFP antibodies (Nyfeler, Michnick et al. 2005) which were used for detecting the protein. PC12 cells were not suitable for analysis due to their smaller size compared to other cell lines.

All constructs were expressed and displayed significant fluorescence after labeling with anti-GFP antibodies, while the empty vector as negative control showed no fluorescence (Figures 2.1A, 2.1F). Neuroserpin WT and RM, PC2 and Furin indicated homogenous intracellular distribution (Figures 2.1B-C, 2.1E, 2.1G), whereas PC1/3 also heavily localized in cell processes of N2A cells (Figure 2.1D).
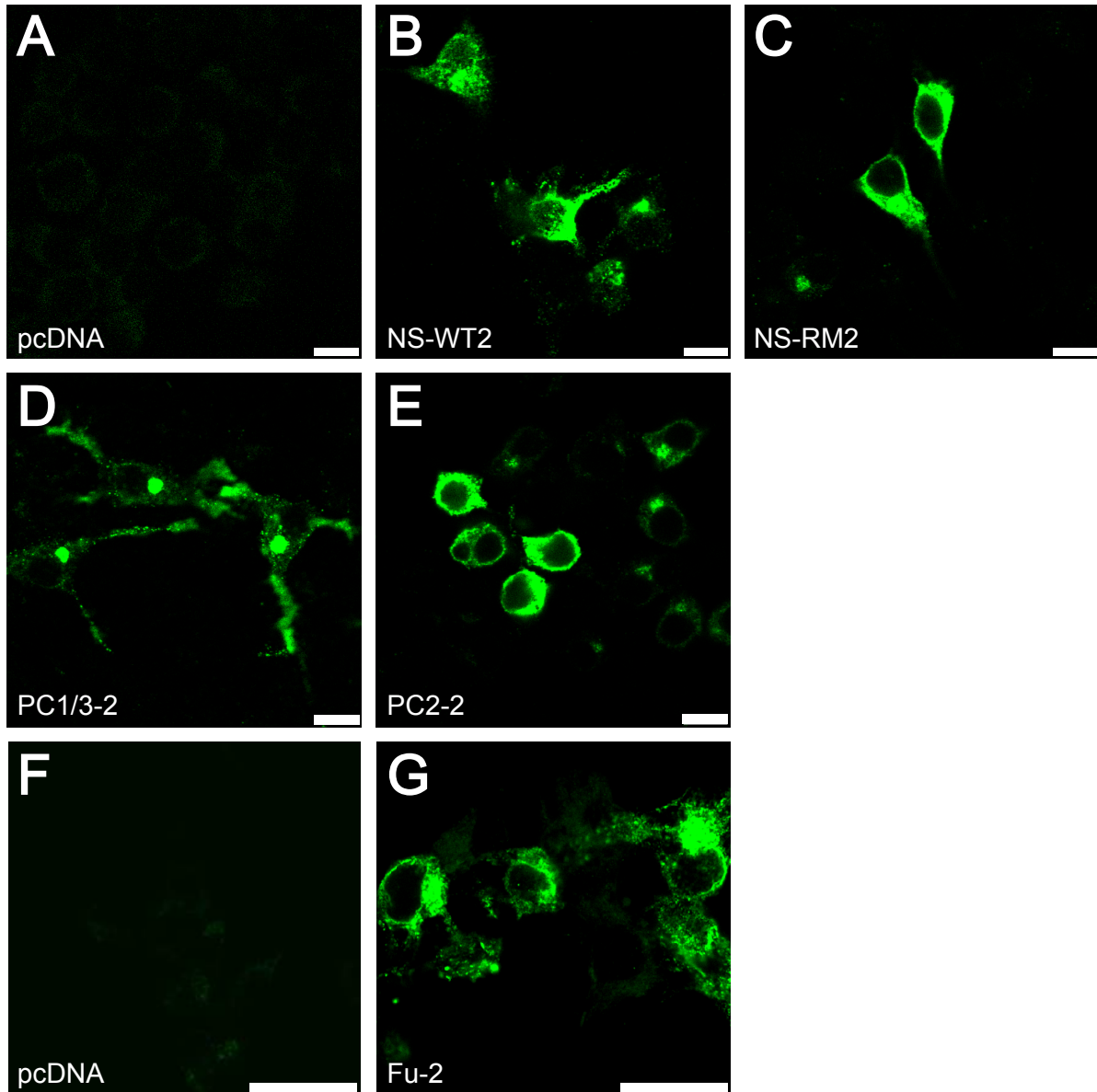
Figure 2.1: Immunofluorescent staining of cells transfected with NS and PCSKs fused to YFP-2 tag. Staining with antiGFP as primary antibody.
(A)-(E): N2A cells transfected with (A): pcDNA, (B): NS-WT2, (C): NS-RM2, (D): PC1/3-2, (E): PC2-2. Scale bar 10μm.
(F)-(G): HEK cells transfected with (F): pcDNA, (G): Fu-2. Scale bar 20μm.

3.2 Testing complex formation by YFP-PCA in HEK and N2A cells

For complementation assays we used the same cell lines (HEK and N2A) as in preceding immunofluorescence experiments. Same constructs were used for transfections as described above. Furthermore, we analyzed truncated Furin ("trFu") for interaction with neuroserpin. This construct represents a version of Furin resulting after physiological ectodomain shedding and it was discovered not to be membrane-bound and soluble (Thomas 2002). tPA, known to complex with neuroserpin *in vitro*, was studied, as well. All mentioned proteins were tagged with YFP-1 or YFP-2 split tags.
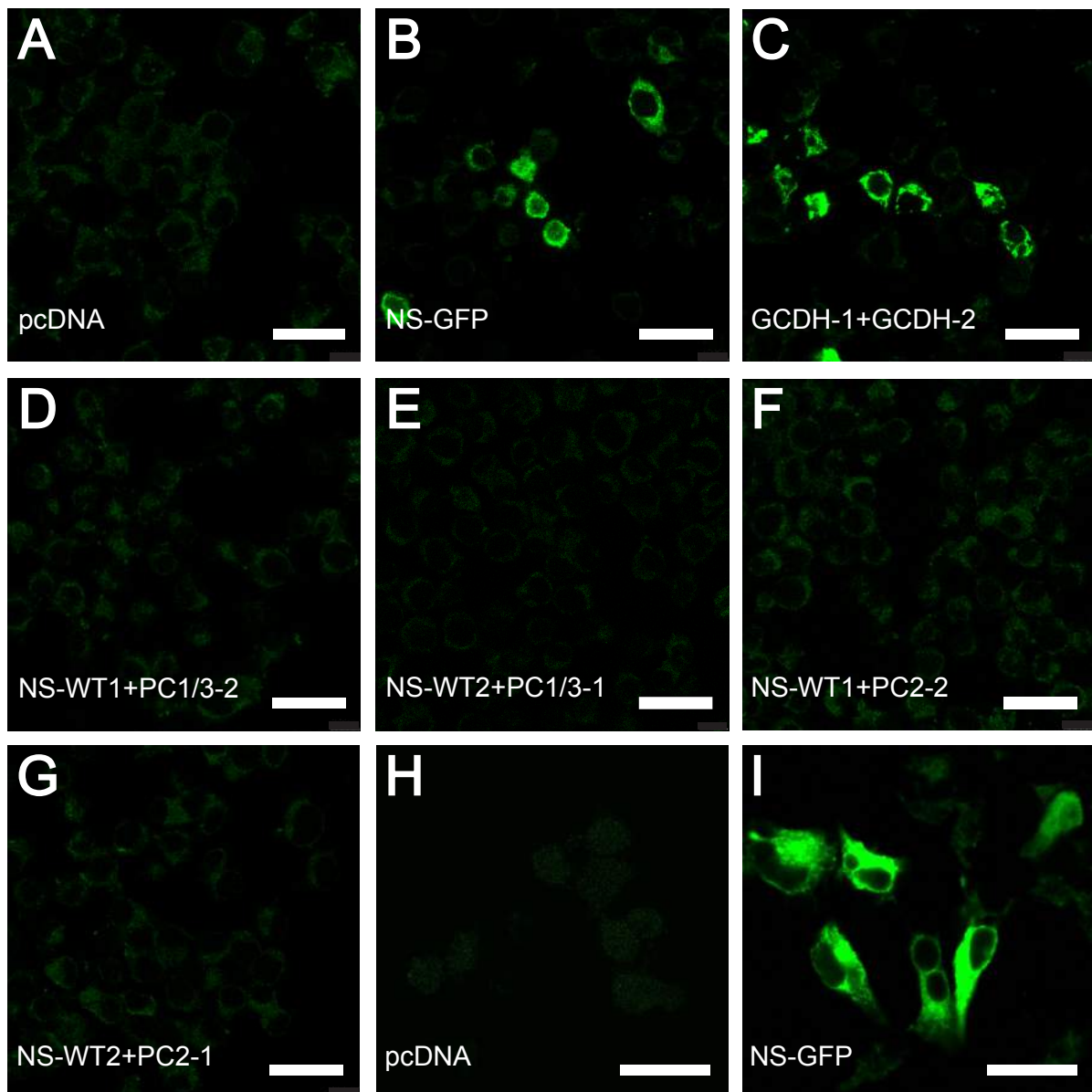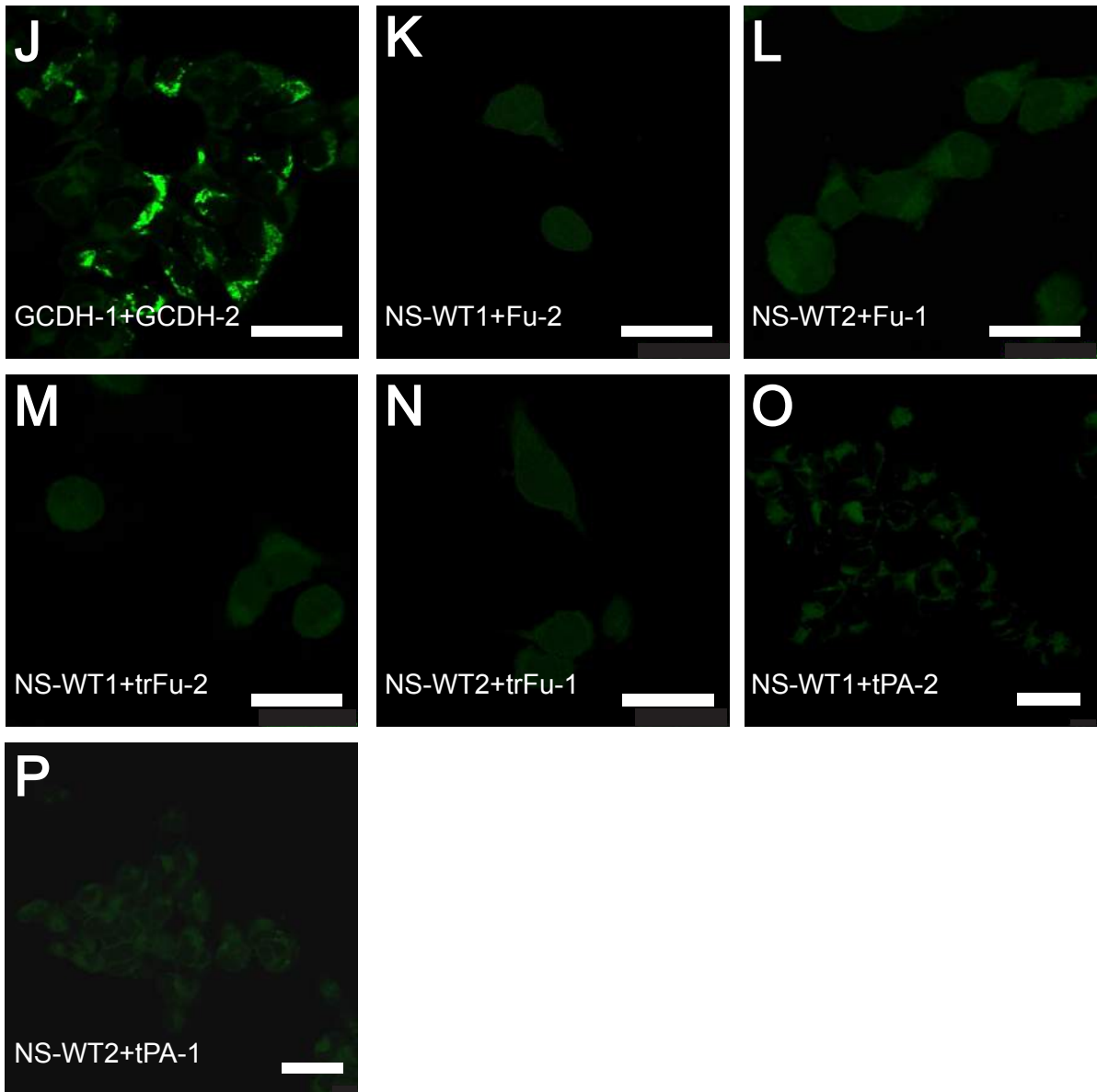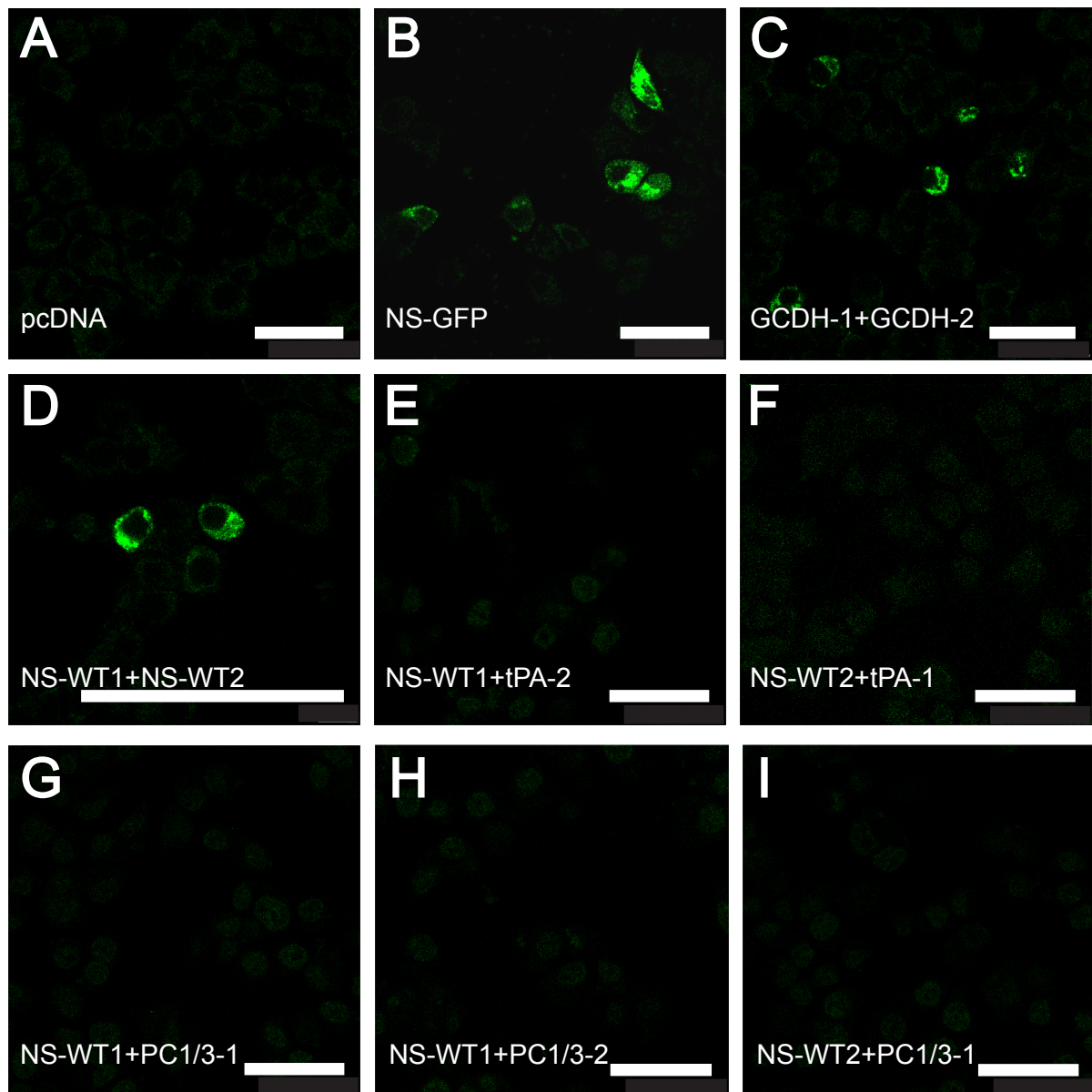
Figure 2.2: YFP-PCA showing lack of interaction between neuroserpin and PC1/3, PC2, Furin and tPA in N2A and HEK cells.
(A)-(G): N2A cells. (H)-(P): HEK cells. Scale bars 25μm.

The positive controls, NS-GFP and GCDH1+2, showed significant fluorescence in HEK and N2A cells (Figures 2.2B-C, 2.2I-J), contrary to the negative control, pcDNA, in both cell lines (Figure 2.2A, 2.2H). Any combinations of neuroserpin and PC1/3 (Figures 2.2D-E), neuroserpin and PC2 (Figures 2.2F-G), neuroserpin and Furin (Figures 2.2K-L), or neuroserpin and truncated Furin (Figures 2.2M-N) did not emit significant fluorescence. Interestingly, after cotransfecting neuroserpin with tPA, the target of neuroserpin we did not detect any signal in protein complementation assay (Figures 2.2O-P). Neuroserpin with mutated reactive site loop (NS-RM) or non complimentary split tag combinations (e.g. YFP-2 with YFP-2) of constructs above were negative [images not shown].

3.3 Testing complex formation by YFP-PCA in cells from adrenal medulla

After obtaining the negative results of the YFP-PCA in HEK and N2A cells we tried to detect interactions by using a different cell line. This cell line consists of neuroendrocrine cells derived from rat pheochromocytoma cells (Greene and Tischler 1976). The technical approach of YFP-PCA in PC12 cells was identical with the YFP-PCA that we applied to N2A and HEK cells.
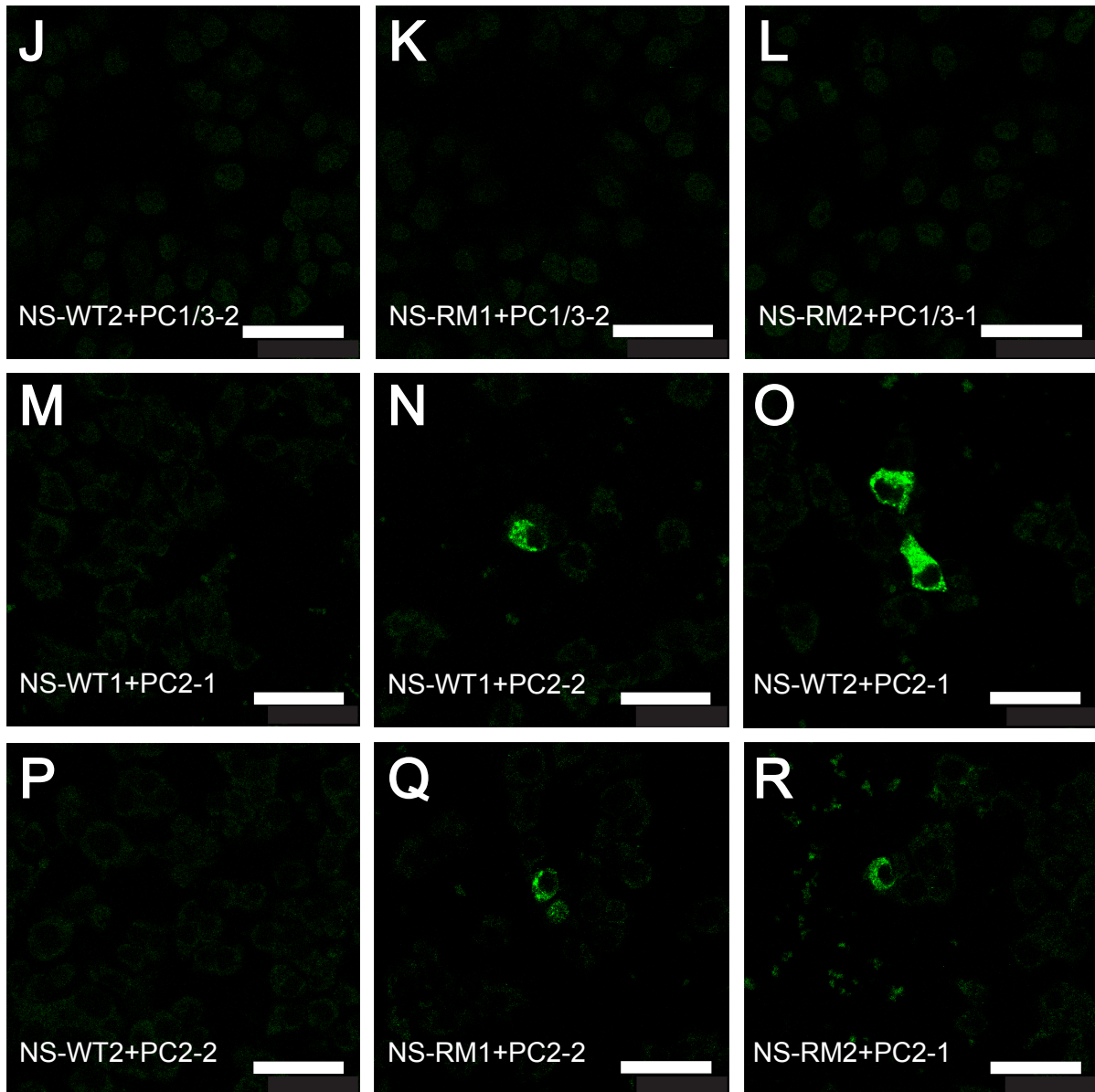
Figure 2.3: YFP-PCA showing interaction between neuroserpin and PC2. (A)-(R): PC12 cells. Scale bar 25μm.

The positive controls, NS-GFP and GCDH1+2, showed significant fluorescence (Figures 2.3B, 2.3C), contrary to the negative control pcDNA (Figure 2.3A). Significant fluorescence was also observed in the contransfections of neuroserpin with PC2 (Figures 2.3N, 2.3O). Surprisingly, signals were also obtained when PC2 had been cotransfected with the reactive loop-mutated neuroserpin NS-RM (Figures 2.3Q, 2.3R). Non-complimentary combinations of neuroserpin and PC-2 did not yield fluorescence (Figures 2.3M, 2.3P). Interestingly, no signals were detected in any cotransfection of tPA with neuroserpin (Figures 2.3E, 2.3F). Any combination of PC1/3 with neuroserpin did not emit fluorescence, as well (Figures 2.3G - 3L). Of particular interest, when the tagged neuroserpin was cotransfected with its

complementary tagged neuroserpin counterpart, it induced YFP fragment complementation (Figure 2.3D).

3.4 Investigation of complex formation by Western blot analysis

In addition to the YFP-PC assay, complex formation between neuroserpin and protease was investigated by cotransfection and Western blot analysis. While in YFP-PCA it is mandatory to have supplementary split tags, in Western blot the fluorescence emission is not needed. Instead, an antibody-coupled reaction is triggered for signal emission. The antibody applied in the following Western blots (antiGFP-Ab) binds to YFP2 (Nyfeler, Michnick et al. 2005). In order to increase the signal, we mainly used proteins that were both tagged with non-complimentary YFP2 tags in double transfections.

At first, to assure that each protein was correctly expressed with the appropriate molecular mass, single transfections were carried out. The YFP-2 tag consists of 240bp with an expected molecular weight of approx. 8kDa which has to be added to the molecular weight of each protein tested. Furin consists of 794 amino acids (Thomas 2002), running in SDS-PAGE at a molecular weight of approx. 110kDa (Figure 2.4).

PC1/3 is synthesized as inactive zymogen with a molecular weight of 99kDa. After removal of the prodomain an intermediate form of 87kDa is produced, that is further cleaved to yield the fully active enzyme at 66kDa (Lindberg, Ahn et al. 1994). A band was observed at approx. 100kDa (Figure 2.4).

The inactive form of PC2 runs at 75kDa, after removal of the prodomain the active form of PC2 is detected at 65kDa (Malide, Seidah et al. 1995). In our experiment, the band of the tagged PC2 was identified at approx. 90kDa (Figure 2.4). Wildtype Neuroserpin has a molecular weight of approx. 50kDa (Hastings, Coleman et al. 1997), in combination with an YFP-2 tag approx. 58kDa altogether. The point mutated negative control NS-RM should have nearly identical weight. Both proteins exhibited bands at approx. 60kDa (Fig. 2.4).
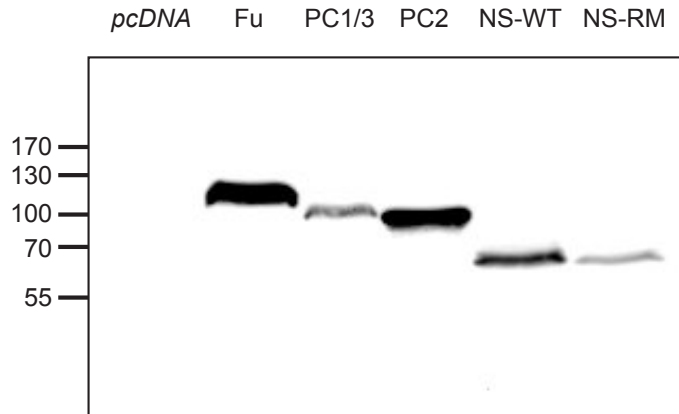
Figure 2.4: Western blot of cell extracts illustrating successful transfection of NS and PCSKs in N2A cells. Proteins fused to YFP-2 tags are detected by antiGFP-antibody.

Since expression of all proteins of interest could be proven, we next tested the complex formation of neuroserpin with different proteases by Western blot. We used tPA, the putative target of neuroserpin as positive control (Osterwalder, Cinelli et al. 1998).
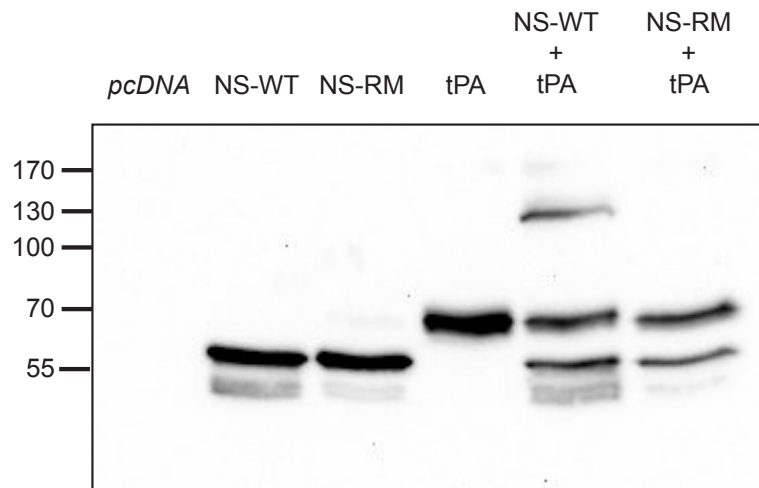

Figure 2.5: Western blot of cell extracts illustrating complex formation between NS and tPA. HEK cells were transfected with NS (WT and RM-mutant) and tPA, both fused to YFP2 tag. Probing the membrane with antiGFP-Ab revealed expression of NS and tPA, as well as a complex at ca. 130kDa in cotransfection with NS-WT. No complex is seen in cotransfection with mutant NS.

Neuroserpin and tPA, both carrying the YFP-2 tag, were co-expressed in HEK cells. NS-WT and NS-RM were expressed at their molecular weight of approx. 60kDa. tPA was expressed at approx. 70kDa which complies with combined masses of the tag (8kDa) and its known molecular weight (66kDa) (Orth, Madison et al. 1992). As expected, when neuroserpin was cotransfected with tPA, a complex was observed at ca. 130kDa. There were no complexes visible with the negative control NS-RM (Figure 2.5).

Finally, we tested the complex formation between neuroserpin and PCSKs.

Neuroserpin and Furin, both with YFP-2 tags, were cotransfected in N2A cells. The cell extracts were collected (1d after transfection), proteins separated by gel electrophoresis and analyzed by Western blot using an antibody against GFP. Beside neuroserpin (wildtype and mutant) at 60kDa, and Furin at 110kDa, a band was observed at >170kDa (Fig. 2.6A).

To investigate if Furin was a component of this band, the blot was stripped and probed with anti-Furin antibodies. The second blot showed bands at the expected size for Furin, whereas no signal was detected at the size of the previously discovered band (Figure 2.6B). The band at approx. 60kDa in the lane of NS-WT represents a neuroserpin signal that was not efficiently stripped after the first hybridization.
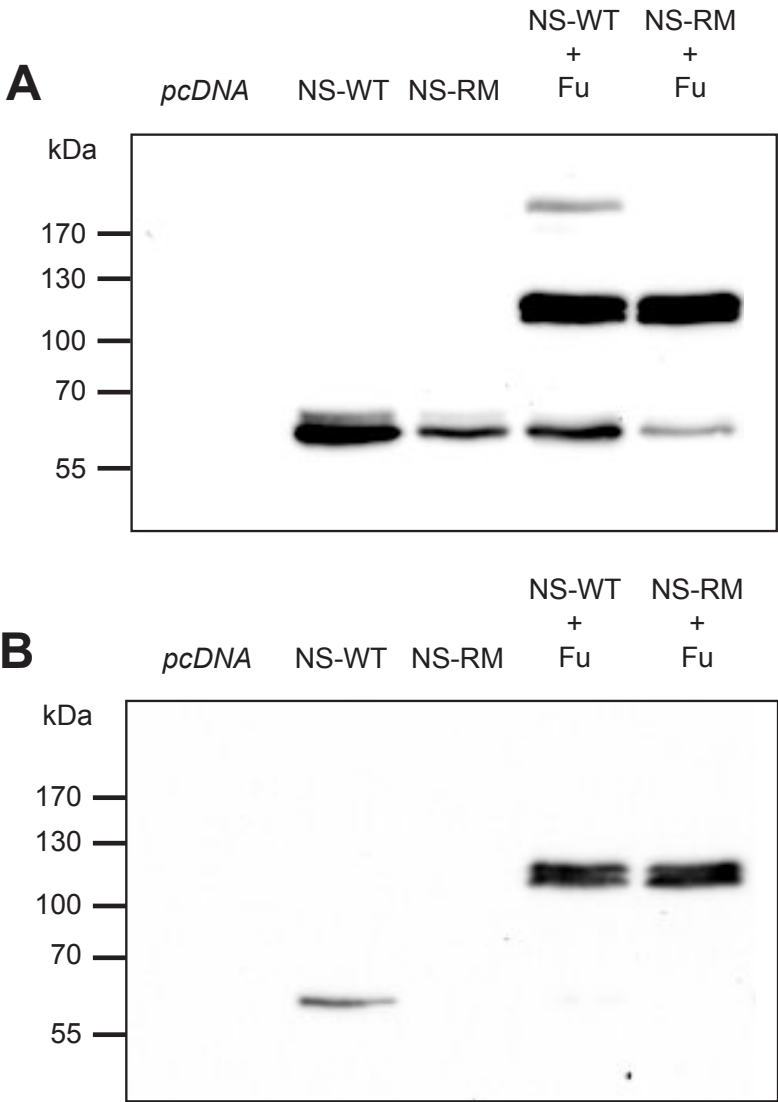

Figure 2.6: Cotransfection of NS with Furin revealed a high-molecular weight band in CE. N2A cells were cotransfected with NS and Furin, both fused to YFP2 tag. Immunoblotting with antiGFP-Ab revealed the presence of a complex at >170kDa in the presence of WT but not RM-mutant NS (A). When probing with antiFurin-Ab, the complex was not detected (B).

To examine if PC1/3 and PC2 will undergo complex formation with neuroserpin, neuroserpin and PC1/3 were cotransfected in HEK cells, whereas neuroserpin and PC2 were cotransfected in N2A cells. 1d after transfection, cell extract was collected, protein separated by gel electrophoresis and analyzed by Western blot using antibody against GFP.

Neuroserpin and PC1/3 were both expressed by HEK cells, but no complex was detected by Western blot (Figure 2.7A). PC2 and neuroserpin were expressed at their appropriate molecular weights by N2A cells, but no band, indicating complex formation with neuroserpin could be observed (Figure 2.7B).
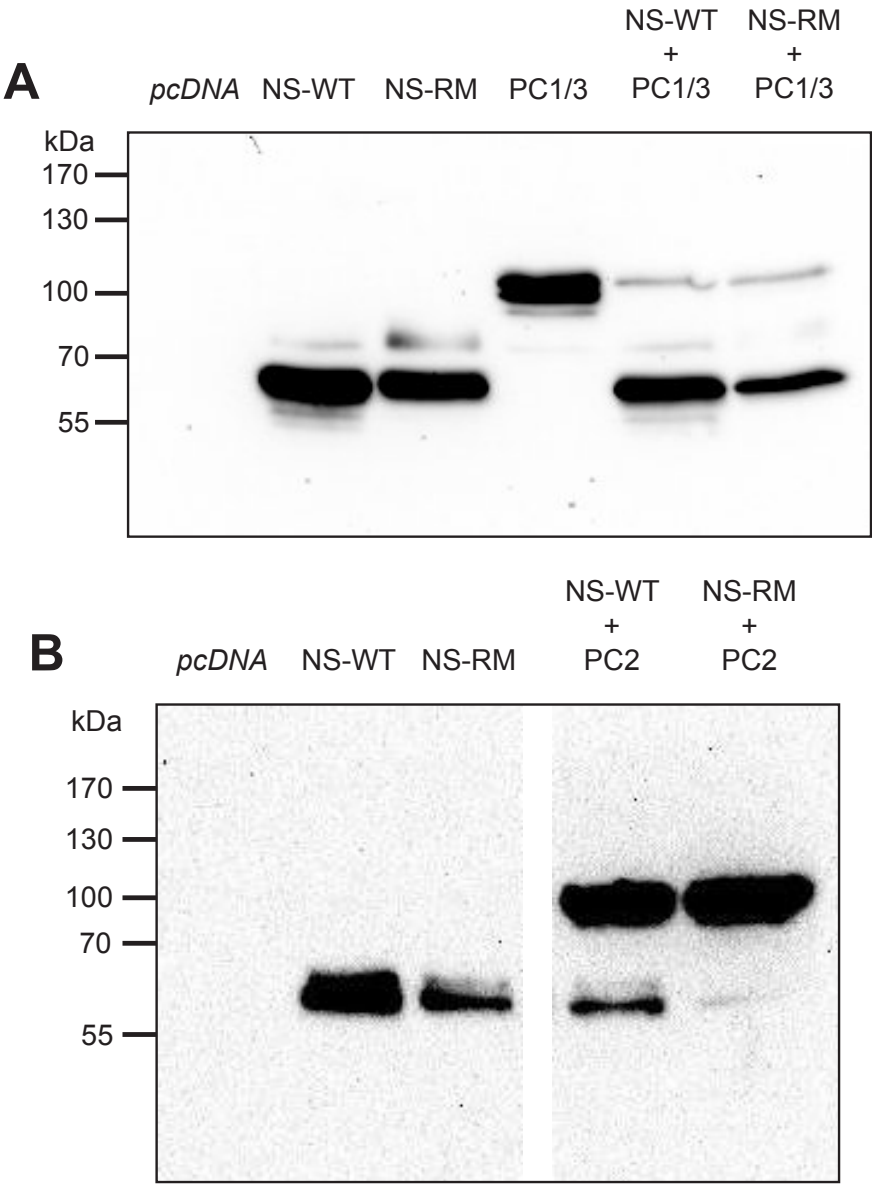

Figure 2.7: Western blots of cell extracts from cells cotransfected with NS and PC1/3 or PC2, all fused to YFP-2 tags. Single and cotransfections of NS and PC1/3 in HEK cells (A) and of NS and PC2 in N2A cells (B). All fusion-proteins could be detected with antiGFP-Ab. No complex could be observed.

3.5 Enrichment of neuroserpin-PC2-cotransfected cells for Western blot analysis

In preceding YFP-PCA, we noticed a complex formation of neuroserpin with PC2. However, in Western blotting we were not able to detect any complex in cotransfection of both proteins. During microscopic analysis of neuroserpin-PC2-cotransfected cells we noticed the overall number of positive cells to be very small when compared to images of any positive control. This led to the assumption that the amount of cells double transfected with neuroserpin and PC2 may have been too low to detect by immuno blot. In order to increase the concentration of successfully cotransfected cells for Western blot analysis, we conducted fluorescence-activated cell sorting (FACS). The sorting of a large number of double transfected PC12 cells should elevate the concentration of positive cells yielded. By using the resulting purified cells we expected to see complex formation of neuroserpin and PC2 by Western blot.
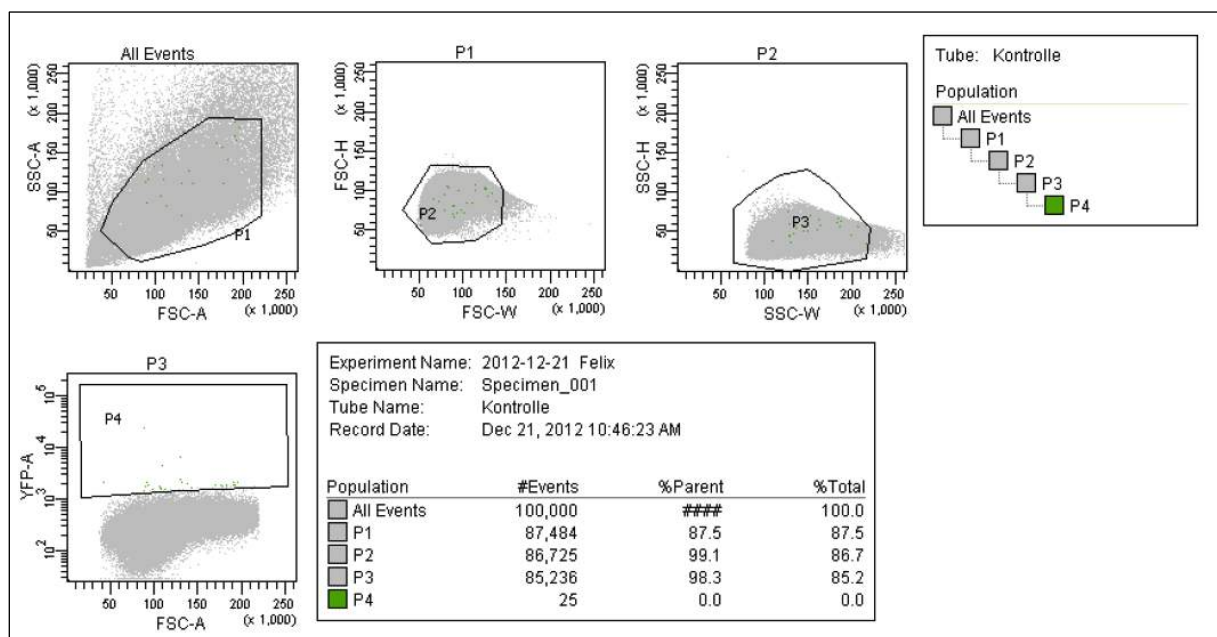

Figure 2.8: FACS sorting of PC12 cells transfected with the negative control pcDNA.
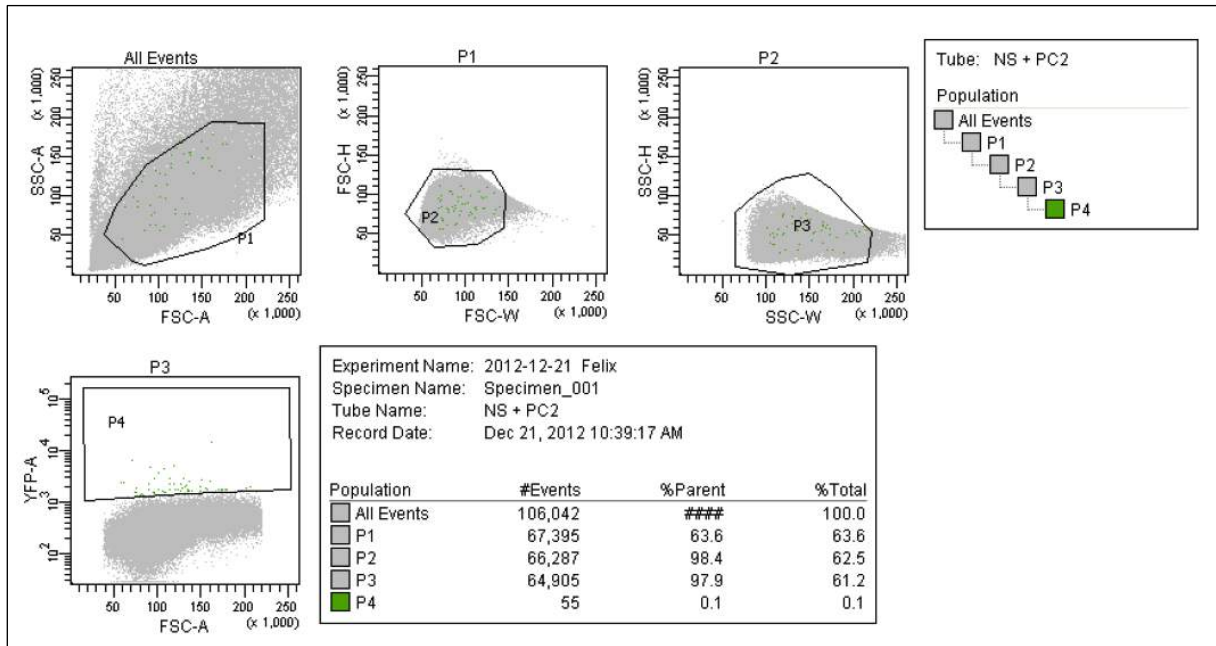
Figure 2.9: FACS sorting of PC12 cells cotransfected with neuroserpin and PC2.

PC12 cells were transfected with the negative control pcDNA or cotransfected with both YFP-2 tagged neuroserpin and PC2. Cells were collected 1d after transfection and FACS was performed with each of the two cell cultures.

FACS did not result in a sufficient high amount of positive cells ($n_{pos} = 0,1\%$) (Figure 2.9). In addition, the falsely positive cells found in the negative control ($n_{pos} < 0,1\%$) were of comparable number (Figure 2.8). Nevertheless, a cell lysate was prepared and analyzed by Western blot.

The Western blot did not reveal any band when probed with antiGFP-Ab (Figure 2.10). However, the positive controls (extract from N2A cells cotransfected with neuroserpin and PC2) revealed the expected bands at approx. 100kDa (PC2) and approx. 60kDa (NS).
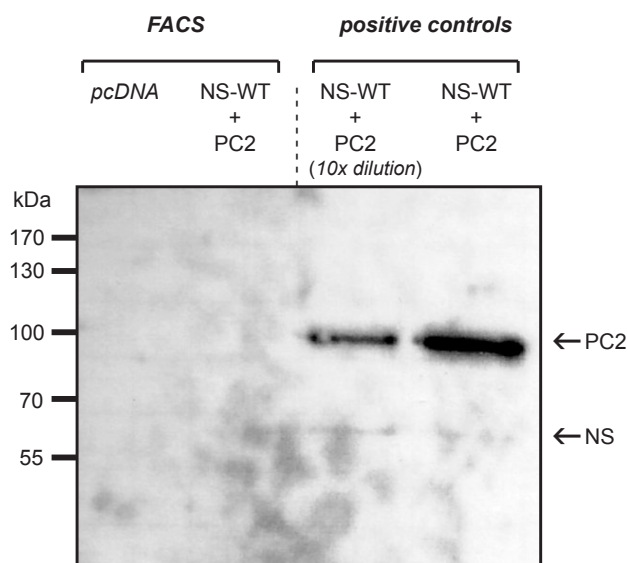
Figure 2.10: Western blot of cell extracts from cells cotransfected with NS and PC2, both fused to YFP-2 tags. Left: lysates from PC12 cells transfected with pcDNA (negative control) or cotransfected with neuroserpin in PC2 and subsequently FACS sorted. Right: lysates from N2A cells cotransfected with neuroserpin and PC2. Outer right lane normally concentrated, inner right lane 10x diluted to compensate for too strong signal.
Fusion-proteins could be detected with antiGFP-Ab in positive controls only. No bands could be observed in lysates from FACS sorted cotransfected cells.

3.6 Analysis of inhibition of PC2 proteolytic activity by neuroserpin

Since neuroserpin has been shown to interact with PC2 in YFP-PCA, we investigated if following complex formation PC2 is inhibited by neuroserpin. PC1/3 and PC2 are key activators in the regulated secretory pathway of endocrine cells. One of the targets that is processed by both proteins is pro-opiomelanocortin (POMC) (Seidah 2011). POMC is cleaved by PC1/3 to yield ß-lipotropin and adrenocorticotropin (ACTH). PC2 cleaves POMC into ß-endorphin and either α-melanotropin (αMSH) or desacetyl-αMSH (Benjannet, Rondeau et al. 1991).

In POMC single transfected N2A cells, an immunoblot should show high levels of POMC when probed with anti-ACTH antibody. By transfecting POMC together with one of its processing proprotein convertases, it should be subject to increased cleaving. This should result in increased levels of its split products including ACTH, which has a lower molecular weight than POMC. By adding neuroserpin DNA in triple transfection, the presence of neuroserpin may lead to inhibition of PC2. Eventually, PC2 becomes disabled in cleaving POMC. In this case, we would rather expect the more full-length POMC as seen in single transfection before.
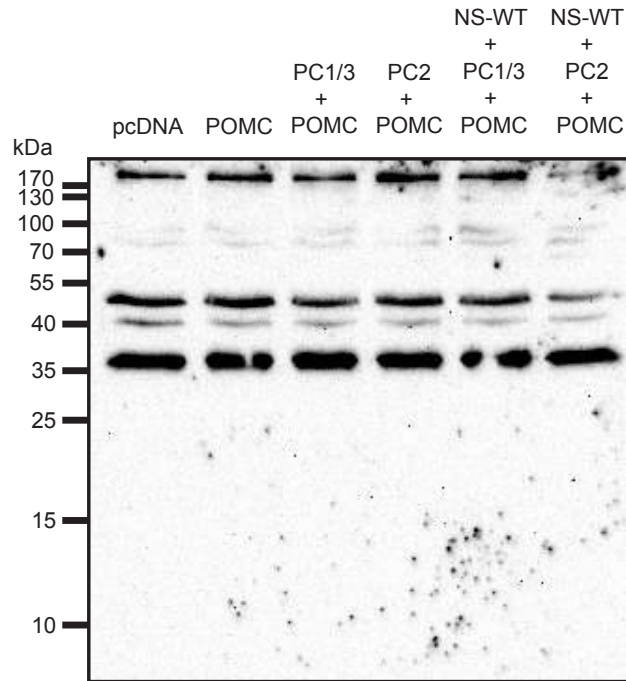
Figure 2.11: Western blot obtained by triple transfection in N2A cells. Probing with anti-ACTH antibody showed characteristic bands of POMC at 36kDa.

To investigate this topic we performed single, double and triple transfections in N2A cells. Transfection with pcDNA served as negative control. A POMC construct was used in single (positive control), double and triple transfections. PC1/3 and PC2, both YFP tagged, were transfected in double and triple transfections. For triple transfections, wild-type neuroserpin construct with YFP tag was added.

After probing with anti-ACTH antibody, the blot did not show any differences between single, double, triple transfection and negative control, indicating that POMC transfection was not successful. Figure 2.11 illustrates that in all lanes a strong signal at ca. 36kDa was detected, which complies with the molecular weight of POMC. However, the intensity of the band was not higher in cells transfected with POMC compared to mock transfected cells. Further, there were bands at ca. 40kDa, 50kDa, 80kDa, 90kDa and >170kDa of unknown specificity. We did not observe any signal within the range of ACTH (6kDa).

3.7 Expression of PC2 inversely correlates with expression of neuroserpin in murine pituitary

To further investigate the relation between neuroserpin and PC2 *in vivo*, we examined the amount of PC2 in pituitaries (n total = 8) of neuroserpin knock-out (KO; n=3), neuroserpin overexpressing transgenic (Tg; n = 2) and wild-type (WT; n = 3) mice. We chose to collect the pituitaries because both neuroserpin and PC2 are expressed at high levels in the neuro-intermediate lobe of mouse pituitary (Marcinkiewicz, Day et al. 1993; Hill, Parmar et al. 2000). Tissue was dissected from mice, suspended in homogenization buffer containing phosphatase inhibitor, homogenized and then solubilized in 1% Triton X100. Probes were separated by SDS-PAGE and analyzed by Western blot.
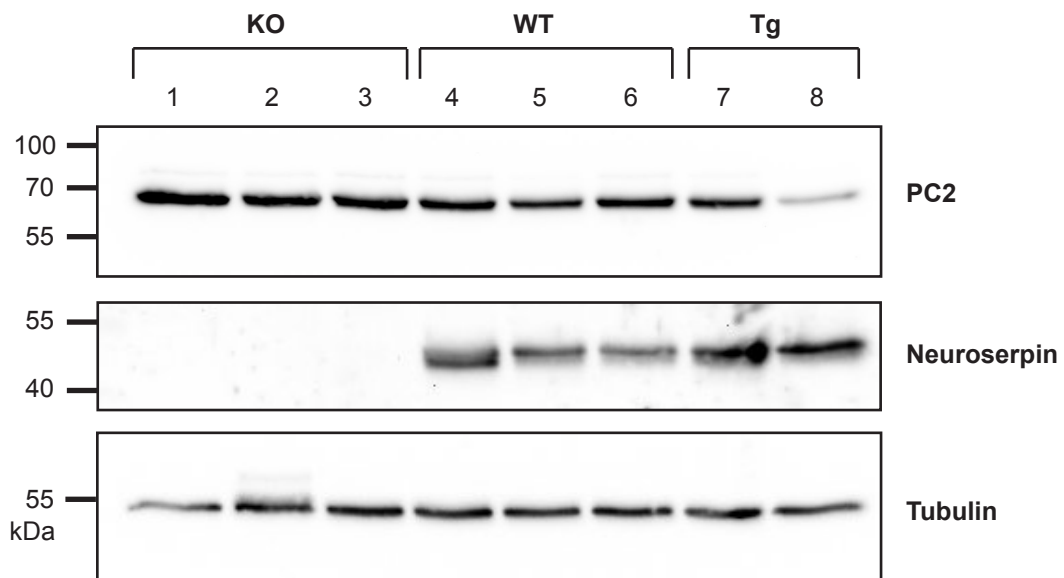
Figure 2.12: Western blot of mice pituitaries (1-8) probed with different antibodies (anti-PC2, anti-Neuroserpin, anti-Tubulin).

As expected, immunoblotting proved presence of neuroserpin in transgenic and wild-type mice only. Tubulin (used as loading control) and PC2 were expressed in all pituitary samples (Figure 2.12). Quantification of the bands on immunoblots (Figure 2.13) revealed a mean value of 0,49 ±0,34 of relative amount of PC2 found in knock-out mice, compared to a lower mean value of 0,25 ±0,03 of relative amount of PC2 found in wild-type mice ($p = 0,299$). Transgenic mice appear to show less presence of PC2, but due to the low number of animals we could not perform statistic analysis.

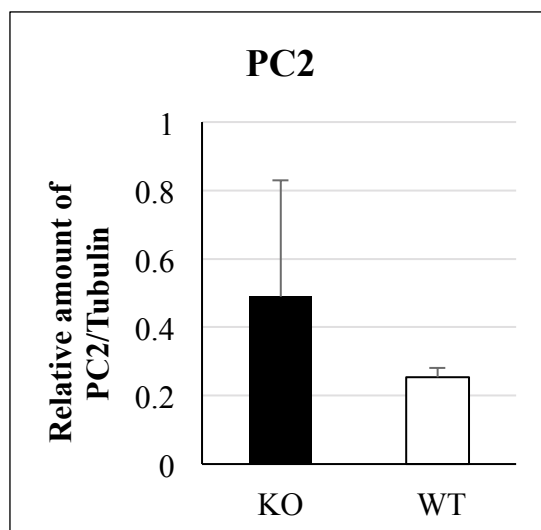*Figure 2.13: Quantification of PC2 protein in KO and WT murine pituitaries.*

3.8 Expression and activity of PC2 in wild-type and neuroserpin knock-out murine brain extract

To analyze the influence of NS on the expression and proteolytic activity of PC2 *in vivo*, we investigated total brain homogenates (n total = 6) of neuroserpin wild-type mice (n = 3) and neuroserpin knock-out mice (n = 3). Brain tissue was obtained from newborn mice (P0) and homogenized using a dounce homogenizer. Proteins were solubilized in 1% Triton X100 and separated by SDS-PAGE. A Western blot membrane was probed using anti-PC2 and anti-ACTH antibodies. The stripped blot probed with anti-Tubulin served as a loading control. All lanes showed valid signals after exposure to each antibody (Figure 2.14). Probing with anti-PC2 showed two bands above and below the 70kDa marker for each lane, which complies with the cited masses of proPC2 (75kDa) and activated PC2 (64kDa) (Shen, Seidah et al. 1993). Exposure to anti-ACTH indicated two bands at approx. 35kDa and 39kDa. Former studies suggest that proACTH precursors (POMC and prePOMC) in mice have molecular weights of 39, 34, 32kDa (Liotta, Loudes et al. 1980). The latter two masses, 34 and 32kDa, were not distinguishable in our blot. Anti-Tubulin showed at approx. 50kDa.
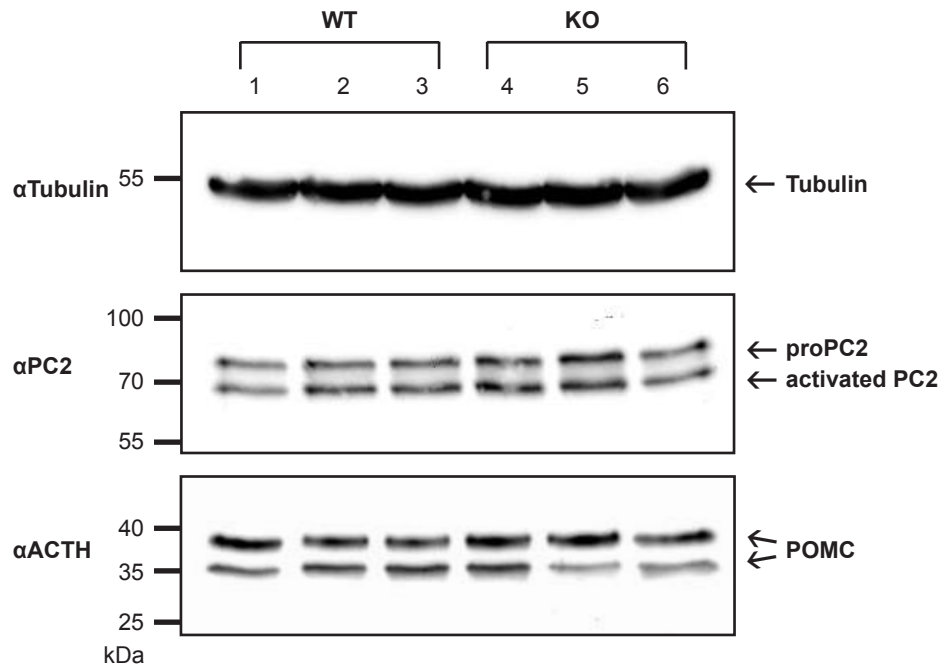
Figure 2.14: Western blot of brain extract probed with anti-Tubulin, anti-PC2 and anti-ACTH antibodies. Wild-type and knock-out groups are indicated on the top.

To evaluate the differences in protein expression, intensity of the bands of PC2 was measured by signal quantification. The lower and the upper bands were quantified separately. In figure 2.15, upper and lower bands are shown separately for either WT or KO. Figure 2.16 presents the combined means of upper and lower signals of each group.

The mean of the relative amounts of proPC2 in wild-type mice was 1,06 ±0,53, while in knock-out mice was 1,54 ±0,40 ($p = 0,280$). Relative amounts of activated PC2 in wild-type mice were calculated as a mean of 1,19 ±0,62; while knock-out mice yielded a mean of 1,70 ±0,51 ($p = 0,335$). Combined mean of the relative amounts of both pro- and activated PC2 was 2,26 ±1,14 in wild-type versus 3,24 ±0,90 in knock-out mice ($p = 0,305$).
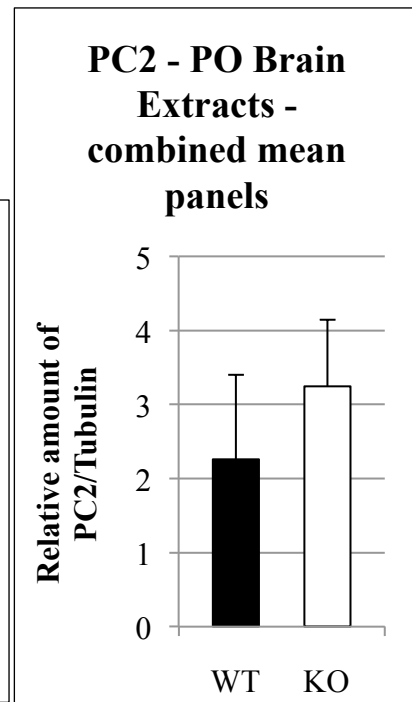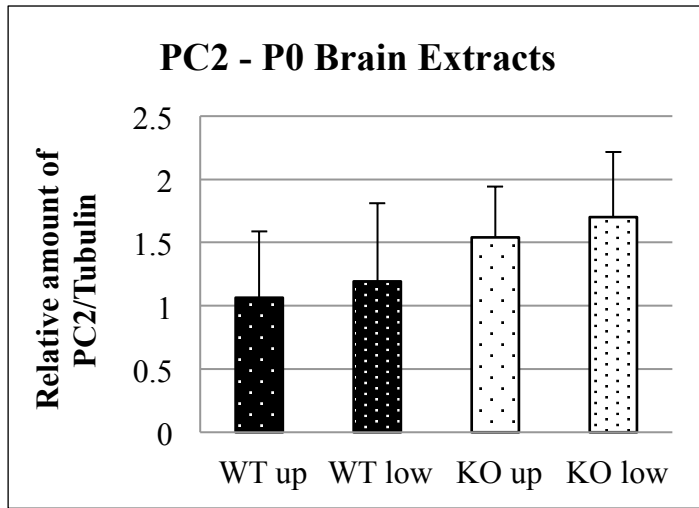
Figures 2.15, 2.16: Comparison of relative amount of PC2 in total brain homogenates of wild-type vs. knock-out mice.

4 Discussion

Neurologic conditions impact people's lives with their disabling course that are costly. The total cost of brain disorders in Europe was €798 billion for the year of 2010, roughly the same as the annual costs of cancer, diabetes and cardiovascular diseases combined together (Gustavsson, Svensson et al. 2011). While the molecular mechanisms differ with every disease, the underlying cause of any neurologic condition includes acute or chronic damage of the central or peripheral nervous system. The time frame in which these conditions develop clinically, ranges from few seconds (e.g., stroke) to many years (e.g., dementia). Yet, once neuronal tissue is damaged there is little recovery. The devastating prognoses of most neurologic diseases warrant a better understanding of their underlying pathomechanisms in order to find the best treatment options.

The expression of neuroserpin is primarily restricted to cells of the nervous system (Hastings, Coleman et al. 1997), where it is known to be involved in the regulation of cell morphology (Hill, Parmar et al. 2000; Parmar, Coates et al. 2002). It is also thought to be involved in embryonic development (Krueger, Ghisu et al. 1997), modulation of synaptic plasticity (Borges, Lee et al. 2010), regeneration (Roet, Franssen et al. 2013) and neurogenesis (Yamada, Takahashi et al. 2010). Studies on genetically modified animals have shown that the overexpression or underexpression of neuroserpin results in an anxiety-like behavior (Madani, Kozlov et al. 2003). Recent studies suggest a role in decision-making (Wong, Ramsey et al. 2012; Wang, Ramsey et al. 2014). Besides its involvement in development, cellular regulation and its psychological features, neuroserpin is known to be neuroprotective in ischemic brain injury and epilepsy (Cinelli, Madani et al. 2001; Yepes, Sandkvist et al. 2002; Gelderblom, Neumann et al. 2013). On the other hand, it promotes survival of cancer cells in brain metastasis (Valiente, Obenauf et al. 2014). Additionally related conditions include Alzheimer's disease and schizophrenia (Hakak, Walker et al. 2001; Kinghorn, Crowther et al. 2006; Brennand, Simone et al. 2011).

Most significant is that the protease inhibitor is prone to polymerization. Mutations in the neuroserpin gene lead to its accumulation in the endoplasmatic reticulum, ultimately causing cell death in a disease called FENIB. While the underlying cause of FENIB is mostly understood, the mechanisms of neuroserpin in the forementioned functions are still disputed. Therefore, it is crucial to understand how neuroserpin carries out its actions and how this

influences the pathways involved (Davis, Shrimpton et al. 1999; Miranda, Romisch et al. 2004).

In the past, many efforts have been made in disclosing the target of neuroserpin *in vivo*. Complex formation with tPA has been described *in vitro* (Krueger, Ghisu et al. 1997; Olson and Gettins 2011). Although neuroserpin's function in inhibiting tPA *in vivo* has been described (Cinelli, Madani et al. 2001; Gelderblom, Neumann et al. 2013), neuroserpin-tPA complex has never been isolated and tPA-independent roles for neuroserpin have been described (Lee, Coates et al. 2008; Wu, Echeverry et al. 2010). As a result, this study hypothesizes that other targets besides tPA might exist. Therefore, the search for neuroserpin target is far from being complete. In this study we chose to investigate three proteins (PC1/3, PC2 and Furin) as likely targets for the following reasons: (1) These proteins are basic residues-cleaving serine proteases that colocalize spatially and temporally with neuroserpin; (2) PC1/3 and Furin are also inhibited by other serpins (alpha1-antitrypsin, alpha1-antitrypsin Pittsburgh, antithrombin); (3) Spn4.1, a Drosophila homolog of neuroserpin, binds to and inhibits soluble human Furin *in vitro* (Osterwalder, Kuhnen et al. 2004).

4.1 YFP-protein fragment complementation assay

Standard methods (e.g., co-immunoprecipitation) have been used in the past to isolate complexes formed between neuroserpin and its target protease. They did not provide any candidates. This is possibly due to the short-lived nature of complexes between neuroserpin and proteases (Barker-Carlson, Lawrence et al. 2002). To circumvent this problem we decided to use the YFP-PC assay, developed to reveal any weak interactions between two proteins within the secretory pathway (Nyfeler, Michnick et al. 2005). The advantage of this method is the stabilization of transient, low-affinity interactions as a result of protein fragment complementation. All of the proteins fused to the YFP fragments (neuroserpin and proteases) were expressed in N2A or HEK cells and could be detected intracellularly (Fig 2.1). Interestingly, we obtained a positive signal when co-expressing two identical neuroserpin molecules; One tagged to YFP fragment 1 and the other tagged to YFP fragment 2 (Figure 2.3 D). This finding is not surprising because neuroserpin is known to self-aggregate (Belorgey, Sharp et al. 2004). Therefore, our results confirm the high-sensitivity of this assay in detecting weak interactions.

4.2 No evidence for complex formation between tPA and neuroserpin in YFP-PCA

Although, some functions of neuroserpin seem to be independent from its role as tPA inhibitor, tPA is still the best characterized target of neuroserpin. Therefore, in this study we used tPA as positive control for YFP-PCA assay. For Western blot analysis, we cotransfected HEK cells with tPA and wild-type neuroserpin that were both fused to YFP2-tags in order to detect both proteins (and the complex originating from them) using an anti-GFP antibody that recognized YFP fragment 2. This resulted in strong bands without background. We noticed a complex of approx. 130kDa (Fig. 2.5). The observed molecular weight corresponds to the combined masses of tagged neuroserpin (approx. 60kDa) and tagged tPA (approx. 70kDa). This complies with previous studies. Moreover, reactive center loop (RCL)-mutated neuroserpin NS-RM did not undergo complex formation with tPA. These results confirm that the expressed proteins functioned properly and that the YFP-tags did not impair complex formation. However, in YFP-PCA assay we did not detect complex formation between neuroserpin and tPA (Fig. 2.2O, 2.2P, 2.3E, 2.3F).

An explanation for why we observed complex formation in Western blot, but not in YFP-PCA, might be attributable to different laboratory steps applied. In order to perform Western blot analysis a lysate of transfected cells must be prepared. By lysing cells, their cellular components are disintegrated and proteins that otherwise would be contained separately are now mixed together. In unlysed cells, tPA and neuroserpin might be confined to different subcellular compartments, while in lysed cells the two proteins might be free to meet and form a complex. In contrast to Western blot, lysate preparation is not part of YFP-PCA. At this point, tPA and neuroserpin would localize to the subcellular compartments that they were directed to. If directed differently, they possibly would not be able to meet and would not undergo complex formation in YFP-PCA.

Another explanation might be that complex formation itself impairs fragment complementation during YFP-PCA. According to suicide substrate mechanism of serpins, a target protease is covalently bound and translocated by 70Å from the top to the bottom of the serpin (Fig. 1.3) (Olson and Gettins 2011). Perhaps the translocation of tPA from one pole to the other of neuroserpin during complex formation also removes the YFP fragments from each other. Trapped in this steric confinement it might be impossible for the YFP-tags to fuse and hence emit detectable signal. For PC2 however, we would not expect to undergo translocation as we speculate PC2 not to bind neuroserpin via reactive center loop (discussed

later). This conclusion is accordant with the observed complex formation of PC2 and neuroserpin in YFP-PCA (Fig. 2.3N, 2.3O, 2.3Q, 2.3R).

4.3 PC1/3 does not undergo complex formation with neuroserpin

When transfecting PC1/3 in N2A cells, we noticed that it is especially localized to cell processes (Fig. 2.1D). Nevertheless, we did not notice complex formation between neuroserpin and PC1/3 in N2A or PC12 cell lines using YFP-PCA (Fig. 2.2D, 2.2E, 2.3J, 2.3K). Accordingly, Western blot analysis failed to prove complex formation in HEK cells (Fig. 2.7A). We conclude that PC1/3 is not a target of neuroserpin.

4.4 Furin does not interact with neuroserpin, but in the presence of Furin neuroserpin undergoes complex formation with an unidentified protein

Since Furin is prevalently active in the constitutive secretory pathway (Thomas 2002), interaction with neuroserpin by YFP-PCA assay was investigated in HEK cells which lack regulated secretion. We tested full-length Furin, as well as a truncated Furin corresponding to the shed form of Furin found extracellularly.

A complex formation between Furin or truncated Furin and neuroserpin in HEK cells was not detected by YFP-PCA. However, when wild-type neuroserpin was cotransfected with Furin in N2A cells and analyzed by Western blot using an anti-GFP antibody we observed a band at >170kDa (Fig. 2.6A). Since both proteins were fused to YFP-tags, we could not differentiate at this point which protein was present in the complex. Moreover, we stripped the membrane and probed it with anti-Furin-Ab, but we could not detect Furin in the complex (Fig. 2.6B). Yet, no band was observed when RCL-mutated neuroserpin was cotransfected with Furin. This suggests that the complex formation occurs via reactive center loop. These results indicate that only in the presence of Furin neuroserpin undergoes complex formation with a third protein via reactive center loop. In conclusion, Furin does not interact with neuroserpin, but possibly activates a substrate which then would undergo a complex formation with neuroserpin. As a result, further experiments are required to characterize the exact composition of this complex.

4.5 PC2 undergoes complex formation with neuroserpin

Cotransfecting wild-type neuroserpin with PC2 in PC12 cells resulted in YFP-complementation (Fig. 2.3N, 2.3O). This was not observed in YFP-PCA in N2A cells (Fig. 2.2F, 2.2G). According to the literature, both proteins localize to secretory granules (Hill, Parmar et al. 2000; Seidah 2011) and PC12 cells that endogenously express higher levels of PCs as compared to N2A, possess an especially efficient mechanism for the activation and targeting of PCs to secretory granules (Lindberg, Ahn et al. 1994). Colocalization is a crucial requirement for any protein-protein interaction. If PC12 cells are adept at targeting PCs as well as neuroserpin to secretory granules, then their concentrations increase within the granules, thus increasing YFP signal in case of fragment complementation. This might explain why we were able to detect YFP signal in cotransfections of neuroserpin and PC2 only in PC12, but not in any different cell lines.

A key feature of serpin suicide substrate mechanism is recognition and binding of the RCL by the target protase. In the first step, the protease recognizes specific residues exposed by the RCL of the serpin, forming a non-covalent Michaelis-like complex. In the second step, the RCL is cleaved by the protease. The protease is then covalently bound to the serpin and translocated to the opposite pole of the serpin, and thereby inhibited (Olson and Gettins 2011).

Since we expect a protease to bind neuroserpin at the reactive site loop, we designed the RCL-mutant as negative control. However, RCL-mutated neuroserpin induced YFP-complementation with PC2 in PC12 cells (Fig. 2.3Q, 2.3R). The introduced mutation in the RCL of neuroserpin was not sufficient in inhibiting recognition or binding by PC2. As a consequence, it was assumed that the interaction takes place at another position.

Moreover, cotransfection and subsequent Western blot analysis did not provide evidence for complexation between neuroserpin and PC2 (Fig. 2.7B). Initially, it was hypothesized that this could be due to the low level of double-transfected cells. To increase the number of such cells we FACS-sorted them. It was evident from FACS protocol that cell sorting did not result in a sufficient high amount of positive cells (Fig. 2.9). Therefore, the complex formation was unobservable (Fig. 2.10). Later, it was realized that since interaction is also achieved with the RCL-mutant of neuroserpin, it can be postulated that this does not lead to the production of a covalent, SDS-stable complex. Usually, SDS-stable complex is observed when a serpin binds its target protease via RCL. Therefore, it is obvious that the interaction between neuroserpin and PC2, observed in YFP-PCA assay, cannot be detected by Western blot since it takes place

at a yet unknown position and is apparently not covalent in nature. Further experiments are currently planned to disclose the exact mechanism of complexation between neuroserpin and PC2.

4.6 Does neuroserpin inhibit PC2 in its proteolytic activity?

At the beginning of this work it was hypothesized that neuroserpin could form complexes with PCs at the reactive center loop and as a consequence it could inhibit their proteolytic activity. To test this, a triple transfection of neuroserpin, protease and substrate was planned to detect the possible influence of neuroserpin on the activity of PCs. As a substrate of PC1/3 and PC2 we chose POMC that is cleaved by both proteases to give rise to ACTH. We cloned POMC in an expression vector and proceeded to triple transfection. This was unsuccessful because overexpression of POMC was not achieved, although sequencing of the construct did not reveal any problems. Moreover, the overexpressed protein of neuroserpin and PC2 could be detected to exclude problems with transfection. Nevertheless, by Western blot we could detect a band for endogenous POMC, but unfortunately not the band for the cleavage product, ACTH. This could be due to the small size of the protein (6 kDa). For that reason, a conclusion could not be obtained concerning neuroserpin-mediated inhibition of PC2. Consequently, attempts were terminated to quantify PC2 activity when we realized that interaction with neuroserpin does not take place at the RCL, so neuroserpin cannot inhibit PC2.

Since neuroserpin and PC2 interact, there was interest in discovering if the expression of both proteins is somehow related. To analyze the relationship between neuroserpin and PC2 *in vivo*, we collected pituitaries from neuroserpin knock-out and wild-type mice. Quantification of immunoblots indicated a tendency toward an inverse correlation between neuroserpin and PC2 protein levels (Fig. 2.13). In neuroserpin deficient animals, PC2 levels were elevated (0,49 ±0,34) in comparison to wild-type animals (0,25 ±0,03). Unfortunately, the finds of this study are not significant as we calculated a p-value of 0,299 ($>$0,05). The low significance could be due to the low number of animals examined (n=3 for KO or WT group). Another problem regarding these results is the high standard deviation in the knock-out group of ±0,34. Subsequently, the low number of examined animals likely contributed to the substandard results. Hence, for future investigations a higher number of animals should be utilized in order to obtain valid observations.

In addition, the expression of PC2 in the brain was also analyzed. In an investigation of murine brain extracts, there was an indication of a tendency towards an inverse relationship between neuroserpin and PC2, as well (Fig. 2.15, 2.16). Since two forms of PC2 were detected (pro-form and active form), both were quantified. Combined mean of pro- and activated PC2 levels in knock-out animals was elevated (3,24 ±0,90) compared to combined mean in wild-type animals (2,26 ±1,14). Yielding an inverse correlation, this finding supports the forementioned relationship in pituitary quantifications. Moreover, the mean relative amount of active PC2 was higher in neuroserpin knock-out mice (1,70 ±0,51) than in wild-type mice (1,19 ±0,62). However, p-values of combined means (p=0,305), means of active PC2 (p=0,335) or means of proPC2 (p=0,280) between animal groups were not significant (>0,05). Besides, we calculated a high standard deviation for every mean value. Good scientific practice forbids drawing any conclusion from non-significant results. Therefore, positive relationships cannot be made concerning the *in vivo* relationship between neuroserpin and PC2. Still, this study detected a tendency towards increased PC2 levels in neuroserpin knock-out animals in both brain and pituitary. Implications for future research should include experiments utilizing a larger sample size of animals. Hopefully, this will lead to lower p-values and possibly more significant results.

The absence of neuroserpin may cause elevated levels of PC2. As a result, it would be interesting to investigate the significance of this finding on POMC cleavage/ACTH production in brain and pituitary. Furthermore, since ACTH could not be detected by Western blot, future experiments will involve improving this step or finding alternatives (e.g. ELISA).

4.7 Implications

In conclusion, a >170kDa neuroserpin-complex was observed by cotransfecting neuroserpin and Furin by SDS-PAGE (Fig. 2.6). YFP-fragment complementation in cotransfections of neuroserpin with PC2 was detected, thus indicating an interaction between the proteins (Fig. 2.3N, 2.3O). In invertebrates, only PC2, 7B2 and neuroserpin are expressed, but not PC1/3 (Seidah, Sadr et al. 2013). This would suggest that there rather is a phylogenetic connection between PC2 and neuroserpin than between PC1/3 and neuroserpin. In fact, the results of this study strongly indicate that PC1/3 does not bind to neuroserpin. Ultimately, follow up research on this topic will help understanding the relevance of these observations.

5 Synopsis

Neuroserpin is a serine protease inhibitor of the central and peripheral nervous system. It is involved in a vast variety of physiologic as well as pathologic pathways. Physiologic functions range from regulation of neuroanatomic properties (e.g., neurogenesis, synaptogenesis and synaptic plasticity) to psychologic properties (e.g., regulation of the emotional state). Neuroserpin is neuroprotective in ischemic brain injury and epilepsy, yet promotes brain metastasis. Most importantly, mutations in the neuroserpin gene lead to a disease called FENIB via accumulation of neuroserpin polymers. While the underlying cause of FENIB is partially understood, the mechanisms by which neuroserpin regulates the forementioned functions are still unknown. *In vitro* data suggest tPA as a target of neuroserpin. However, tPA-neuroserpin complexes have never been isolated *in vivo* and tPA-independent roles for neuroserpin have been described.

In this study, it was hypothesized that other targets besides tPA might exist. As a result, the three proteins including PC1/3, PC2 and Furin were investigated as likely targets. Due to the short-lived nature of complexes between neuroserpin and proteases, the YFP-protein fragment complementation assay was performed providing a method that enables detection of even weak or transient interactions between two proteins.

Results from this study revealed YFP-fragment complementation in cotransfections of neuroserpin with PC2, indicating interaction between the proteins. No interaction was observed in cotransfections of neuroserpin with PC1/3 or neuroserpin with Furin. However, a >170kDa neuroserpin-complex by Western blot analysis was observed when cotransfecting neuroserpin and Furin. This strongly suggests that this complex consists of neuroserpin and an unidentified protein, which possibly is activated by Furin. To further analyze the *in vivo* relationship between neuroserpin and PC2, the protein expression was quantified in pituitary and whole brain homogenates of neuroserpin knock-out and wild-type animals. This showed a tendency toward an inverse correlation between neuroserpin and PC2 protein levels. Follow up research will help to disclose the molecular mechanisms and further understand the relevance of these observations.

6 Appendix

Abbreviations

°C	degree Celsius
€	Euro
3D	three-dimensional
Å	Ångström (1×10^{-10} of a meter)
Ab	antibody
ACTH	adrenocorticotropic hormone
ADAMTS	a disintegrin and metalloproteinase with thrombospondin motifs
AP-2	activating protein 2 (transcription factors)
APP	amyloid precursor protein
approx.	approximately
APS	ammonium persulfate
Arg	arginine
Aβ	amyloid beta
bp	base pair
Ca^{2+}	calcium ion
CAAT	core promoter element
cAMP	cyclic adenosine monophosphate
cDNA	complementary DNA
CE	cell extract
CLIP	corticotropin-like intermediate peptide
CNS	central nervous system
d	day
dansyl-EGR-CMK	dansyl-Glu-Gly-Arg chloromethyl ketone
dist. H_2O	purified water
DMEM	Dulbecco's modified Eagle's medium
DNA	deoxyribonucleic acid
DRG	dorsal root ganglion
E	embryonic day
EcoR1	(restriction enzyme)
ELISA	enzyme-linked immunosorbent assay

ER	endoplasmatic reticulum
FACS	fluorescence-activated cell sorting
FBS	fetal bovine serum
FCS	fetal calf serum
FENIB	familial encephalopathy with neuroserpin inclusion bodies
Fig.	figure
FLAG-	FLAG octapeptide protein tag
Fu	Furin
g	gram
g	gravitational force
GCDH	glutaryl-CoA dehydrogenase
GFP	green fluorescent protein
h	hour
HCl	hydrogen chloride
HEK	human embryonic kidney (cell line)
HindIII	(restriction enzyme)
hiPSC	human induced pluripotent stem cell
HIV-1	human immunodeficiency virus 1
HS	horse serum
HSG	modified Hoagland's solution
HuD	embrionic lethal abnormal vision-like protein 4
Immunofl.	immunofluorescence
Inr	initiator element (core promoter element)
K_2HPO_4	dipotassium phosphate
kcal	kilocalorie (=1000 calories)
KCl	potassium chloride
kDa	kilo Dalton (=1000 Dalton)
KH_2PO_4	monopotassium phosphate
KO	knock-out
l	liter
L1CAM	L1 cellular adhesion molecule
LDL	low-density lipoprotein
low	lower bands
LRP	low density lipoprotein receptor-related protein

m	meter
mA	milliampere
MgSO$_4$	magnesium sulfate
min	minute
mM	millimole
MMP-9	matrix-metalloproteinase-9
mol	mole
mRNA	messenger RNA
n	number
N2A	neuro-2a (neuroblastoma cell line)
NaCl	sodium chloride
NaOH	sodium hydroxide
NGF-γ	nerve growth factor-γ
nm	nanometer (1×10^{-9} of a meter)
NMDA	*N*-methyl-D-aspartic acid
NS	neuroserpin
NS-GFP	neuroserpin with non-fragmented GFP (positive control)
NS-RM	reactive center loop mutated neuroserpin (negative control)
NS-WT	neuroserpin wild-type
OECs	olfactory ensheathing cells
olf-1	olfactoryy receptor 5I1
ONL	olfactory nerve layer
p	*p*-value
P0	perinatally
PA	plasminogen activator
PACE	paired basic amino acid cleaving enzyme
PAI-1	plasminogen activator inhibitor-1
PAS	periodic acid-Schiff
PBS	phosphate buffered saline
PC	proprotein convertase
PC12	rat pheochromocytoma (cell line)
PCA	protein complementation assay
pcDNA	mammalian expression vector
Pcsk	proprotein convertase subtilisin/kexin

pDNR-LIB	(commercially available donor vector)
pH	potentia hydrogenii
PN-1	nexin-1
PNS	peripheral nervous system
POMC	pro-opiomelanocortin
r.m.s.d.	root-mean-square-deviation
rcf	relative centrifugal force
RCL	reactive center loop
RGMa	repulsive guidance molecule
RNA	ribonucleic acid
RSL	reactive site loop
RSV	respiratory syncytial virus
SD	standard deviation
SDS-PAGE	sodium dodecyl sulfate polyacrylamide gel electrophoresis
Ser	serine
serpin	serine protease inhibitor
SERPINI1	neuroserpin
SERPINI2	Pancpin
SI	stoichiometry of inhibition
Sp1	specifity protein 1 (transcription factor)
$t_{1/2}$	half-life
T3	triiodothyronine
TATA	Goldberg-Hogness box (core promoter element)
TBS	tris buffered saline
TEF	thyrotrophic embryonic factor (transcription factor)
TEMED	tetramethylethylenediamine
Tg	transgenic
TGF-β	transforming growth factor beta
TGN	*trans*-Golgi-network
tPA	tissue-type plasminogen activator
trFu	truncated Furin
Tris	tris(hydroxymethyl)aminomethane
up	upper bands
uPA	urokinase plasminogen activator

UTR	untranslated region
V	volt
VLDL	very-low-density lipoprotein
WB	western blot
WT	wild-type
YFP	yellow fluorescent protein
α	anti-
α-MSH	α-melanocyte-stimulating hormone
$α_1$PI	$α_1$-proteinase inhibitor
β-LPH	β-lipotropic hormone
μg	microgram (1×10^{-6} of a gram)
μl	microliter (1×10^{-6} of a liter)
μm	micrometer (1×10^{-6} of a meter)

List of figures

List of tables

7 References

Akassoglou, K., K. W. Kombrinck, et al. (2000). "Tissue plasminogen activator-mediated fibrinolysis protects against axonal degeneration and demyelination after sciatic nerve injury." J Cell Biol **149**(5): 1157-1166.

Barker-Carlson, K., D. A. Lawrence, et al. (2002). "Acyl-enzyme complexes between tissue-type plasminogen activator and neuroserpin are short-lived in vitro." J Biol Chem **277**(49): 46852-46857.

Belorgey, D., J. A. Irving, et al. (2011). "Characterisation of serpin polymers in vitro and in vivo." Methods **53**(3): 255-266.

Belorgey, D., L. K. Sharp, et al. (2004). "Neuroserpin Portland (Ser52Arg) is trapped as an inactive intermediate that rapidly forms polymers: implications for the epilepsy seen in the dementia FENIB." Eur J Biochem **271**(16): 3360-3367.

Benarroch, E. E. (2007). "Tissue plasminogen activator: beyond thrombolysis." Neurology **69**(8): 799-802.

Benchenane, K., V. Berezowski, et al. (2005). "Tissue-type plasminogen activator crosses the intact blood-brain barrier by low-density lipoprotein receptor-related protein-mediated transcytosis." Circulation **111**(17): 2241-2249.

Benjannet, S., N. Rondeau, et al. (1991). "PC1 and PC2 are proprotein convertases capable of cleaving proopiomelanocortin at distinct pairs of basic residues." Proc Natl Acad Sci U S A **88**(9): 3564-3568.

Benjannet, S., N. Rondeau, et al. (1993). "Comparative biosynthesis, covalent post-translational modifications and efficiency of prosegment cleavage of the prohormone convertases PC1 and PC2: glycosylation, sulphation and identification of the intracellular site of prosegment cleavage of PC1 and PC2." Biochem J **294 (Pt 3)**: 735-743.

Berger, P., S. V. Kozlov, et al. (1999). "Neuronal depolarization enhances the transcription of the neuronal serine protease inhibitor neuroserpin." Mol Cell Neurosci **14**(6): 455-467.

Berger, P., S. V. Kozlov, et al. (1998). "Structure of the mouse gene for the serine protease inhibitor neuroserpin (PI12)." Gene **214**(1-2): 25-33.

Beringer, D. X., M. J. Fischer, et al. (2013). "Tissue-type plasminogen activator binds to Abeta and AIAPP amyloid fibrils with multiple domains." Amyloid **20**(2): 113-121.

Berta, T., Y. C. Liu, et al. (2013). "Tissue plasminogen activator contributes to morphine tolerance and induces mechanical allodynia via astrocytic IL-1beta and ERK signaling in the spinal cord of mice." Neuroscience **247**: 376-385.

Bicknell, A. B. (2008). "The tissue-specific processing of pro-opiomelanocortin." J Neuroendocrinol **20**(6): 692-699.

Bode, W. and M. Renatus (1997). "Tissue-type plasminogen activator: variants and crystal/solution structures demarcate structural determinants of function." Curr Opin Struct Biol **7**(6): 865-872.

Borges, V. M., T. W. Lee, et al. (2010). "Neuroserpin regulates the density of dendritic protrusions and dendritic spine shape in cultured hippocampal neurons." J Neurosci Res **88**(12): 2610-2617.

Brennand, K. J., A. Simone, et al. (2011). "Modelling schizophrenia using human induced pluripotent stem cells." Nature **473**(7346): 221-225.

Briand, C., S. V. Kozlov, et al. (2001). "Crystal structure of neuroserpin: a neuronal serpin involved in a conformational disease." FEBS Lett **505**(1): 18-22.

Campenot, R. B. (1977). "Local control of neurite development by nerve growth factor." Proc Natl Acad Sci U S A **74**(10): 4516-4519.

Chang, W. S., N. T. Chang, et al. (2000). "Tissue-specific cancer-related serpin gene cluster at human chromosome band 3q26." Genes Chromosomes Cancer **29**(3): 240-255.

Cinelli, P., R. Madani, et al. (2001). "Neuroserpin, a neuroprotective factor in focal ischemic stroke." Mol Cell Neurosci **18**(5): 443-457.

Collen, D. and H. R. Lijnen (2009). "The tissue-type plasminogen activator story." Arterioscler Thromb Vasc Biol **29**(8): 1151-1155.

Croissandeau, G., F. Wahnon, et al. (2006). "Increased stress-induced analgesia in mice lacking the proneuropeptide convertase PC2." Neurosci Lett **406**(1-2): 71-75.

Cuadrado, A., C. Navarro-Yubero, et al. (2002). "HuD binds to three AU-rich sequences in the 3'-UTR of neuroserpin mRNA and promotes the accumulation of neuroserpin mRNA and protein." Nucleic Acids Res **30**(10): 2202-2211.

Cuadrado, A., C. Navarro-Yubero, et al. (2003). "Neuronal HuD gene encoding a mRNA stability regulator is transcriptionally repressed by thyroid hormone." J Neurochem **86**(3): 763-773.

Davis, R. L., A. E. Shrimpton, et al. (1999). "Familial dementia caused by polymerization of mutant neuroserpin." Nature **401**(6751): 376-379.

de Groot, D. M., C. Pol, et al. (2005). "Comparative analysis and expression of neuroserpin in Xenopus laevis." Neuroendocrinology **82**(1): 11-20.

Dobo, J. and P. G. Gettins (2004). "alpha1-Proteinase inhibitor forms initial non-covalent and final covalent complexes with elastase analogously to other serpin-proteinase pairs, suggesting a common mechanism of inhibition." J Biol Chem **279**(10): 9264-9269.

Doucette, R. (1991). "PNS-CNS transitional zone of the first cranial nerve." J Comp Neurol **312**(3): 451-466.

Elliott, P. R., D. A. Lomas, et al. (1996). "Inhibitory conformation of the reactive loop of alpha 1-antitrypsin." Nat Struct Biol **3**(8): 676-681.

Fabbro, S., K. Schaller, et al. (2011). "Amyloid-beta levels are significantly reduced and spatial memory defects are rescued in a novel neuroserpin-deficient Alzheimer's disease transgenic mouse model." J Neurochem **118**(5): 928-938.

Gagnon, J., J. Mayne, et al. (2009). "Expression of PCSK1 (PC1/3), PCSK2 (PC2) and PCSK3 (furin) in mouse small intestine." Regul Pept **152**(1-3): 54-60.

Galliciotti, G., M. Glatzel, et al. (2007). "Accumulation of mutant neuroserpin precedes development of clinical symptoms in familial encephalopathy with neuroserpin inclusion bodies." Am J Pathol **170**(4): 1305-1313.

Galliciotti, G. and P. Sonderegger (2006). "Neuroserpin." Front Biosci **11**: 33-45.

Gelderblom, M., M. Neumann, et al. (2013). "Deficiency in serine protease inhibitor neuroserpin exacerbates ischemic brain injury by increased postischemic inflammation." PLoS One **8**(5): e63118.

Gettins, P. G. (2002). "Serpin structure, mechanism, and function." Chem Rev **102**(12): 4751-4804.

Greene, L. A. and A. S. Tischler (1976). "Establishment of a noradrenergic clonal line of rat adrenal pheochromocytoma cells which respond to nerve growth factor." Proc Natl Acad Sci U S A **73**(7): 2424-2428.

Gustavsson, A., M. Svensson, et al. (2011). "Cost of disorders of the brain in Europe 2010." Eur Neuropsychopharmacol **21**(10): 718-779.

Hagen, M. C., J. R. Murrell, et al. (2011). "Encephalopathy with neuroserpin inclusion bodies presenting as progressive myoclonus epilepsy and associated with a novel mutation in the Proteinase Inhibitor 12 gene." Brain Pathol **21**(5): 575-582.

Hakak, Y., J. R. Walker, et al. (2001). "Genome-wide expression analysis reveals dysregulation of myelination-related genes in chronic schizophrenia." Proc Natl Acad Sci U S A **98**(8): 4746-4751.

Harbeck, N., C. Thomssen, et al. (1999). "Invasion marker PAI-1 remains a strong prognostic factor after long-term follow-up both for primary breast cancer and following first relapse." Breast Cancer Res Treat **54**(2): 147-157.

Hastings, G. A., T. A. Coleman, et al. (1997). "Neuroserpin, a brain-associated inhibitor of tissue plasminogen activator is localized primarily in neurons. Implications for the regulation of motor learning and neuronal survival." J Biol Chem **272**(52): 33062-33067.

Hedstrom, L. (2002). "Serine protease mechanism and specificity." Chem Rev **102**(12): 4501-4524.

Hill, R. M., P. K. Parmar, et al. (2000). "Neuroserpin is expressed in the pituitary and adrenal glands and induces the extension of neurite-like processes in AtT-20 cells." Biochem J **345 Pt 3**: 595-601.

Hoylaerts, M., D. C. Rijken, et al. (1982). "Kinetics of the activation of plasminogen by human tissue plasminogen activator. Role of fibrin." J Biol Chem **257**(6): 2912-2919.

Hughes, A. M., B. J. Everitt, et al. (1988). "The effects of simultaneous or separate infusions of some pro-opiomelanocortin-derived peptides (beta-endorphin, melanocyte stimulating hormone, and corticotrophin-like intermediate polypeptide) and their acetylated derivatives upon sexual and ingestive behaviour of male rats." Neuroscience **27**(2): 689-698.

Hwang, E. M., S. K. Kim, et al. (2006). "Furin is an endogenous regulator of alpha-secretase associated APP processing." Biochem Biophys Res Commun **349**(2): 654-659.

Irving, J. A., U. I. Ekeowa, et al. (2011). "The serpinopathies studying serpin polymerization in vivo." Methods Enzymol **501**: 421-466.

Irving, J. A., R. N. Pike, et al. (2000). "Phylogeny of the serpin superfamily: implications of patterns of amino acid conservation for structure and function." Genome Res **10**(12): 1845-1864.

Irving, J. A., P. J. Steenbakkers, et al. (2002). "Serpins in prokaryotes." Mol Biol Evol **19**(11): 1881-1890.

Ishigami, S., M. Sandkvist, et al. (2007). "Identification of a novel targeting sequence for regulated secretion in the serine protease inhibitor neuroserpin." Biochem J **402**(1): 25-34.

Iulita, M. F., S. Do Carmo, et al. (2014). "Nerve growth factor metabolic dysfunction in Down's syndrome brains." Brain **137**(Pt 3): 860-872.

Kennedy, S. A., A. C. van Diepen, et al. (2007). "Expression of the serine protease inhibitor neuroserpin in cells of the human myeloid lineage." Thromb Haemost **97**(3): 394-399.

Kiefer, M. C., J. E. Tucker, et al. (1991). "Identification of a second human subtilisin-like protease gene in the fes/fps region of chromosome 15." DNA Cell Biol **10**(10): 757-769.

Kinghorn, K. J., D. C. Crowther, et al. (2006). "Neuroserpin binds Abeta and is a neuroprotective component of amyloid plaques in Alzheimer disease." J Biol Chem **281**(39): 29268-29277.

Knipe, L., A. Meli, et al. (2010). "A revised model for the secretion of tPA and cytokines from cultured endothelial cells." Blood **116**(12): 2183-2191.

Kounnas, M. Z., F. C. Church, et al. (1996). "Cellular internalization and degradation of antithrombin III-thrombin, heparin cofactor II-thrombin, and alpha 1-antitrypsin-trypsin complexes is mediated by the low density lipoprotein receptor-related protein." J Biol Chem **271**(11): 6523-6529.

Krueger, S. R., G. P. Ghisu, et al. (1997). "Expression of neuroserpin, an inhibitor of tissue plasminogen activator, in the developing and adult nervous system of the mouse." J Neurosci **17**(23): 8984-8996.

Kruithof, E. K. and S. Dunoyer-Geindre (2014). "Human tissue-type plasminogen activator." Thromb Haemost **112**(2).

Lamp, J., B. Keyser, et al. (2011). "Glutaric aciduria type 1 metabolites impair the succinate transport from astrocytic to neuronal cells." J Biol Chem **286**(20): 17777-17784.

Lee, R., P. Kermani, et al. (2001). "Regulation of cell survival by secreted proneurotrophins." Science **294**(5548): 1945-1948.

Lee, S. N., D. H. Lee, et al. (2013). "Overexpressed proprotein convertase 1/3 induces an epithelial-mesenchymal transition in airway epithelium." Eur Respir J **42**(5): 1379-1390.

Lee, T. W., L. C. Coates, et al. (2008). "Neuroserpin regulates N-cadherin-mediated cell adhesion independently of its activity as an inhibitor of tissue plasminogen activator." J Neurosci Res **86**(6): 1243-1253.

Lindberg, I., S. C. Ahn, et al. (1994). "Cellular distributions of the prohormone processing enzymes PC1 and PC2." Mol Cell Neurosci **5**(6): 614-622.

Liotta, A. S., C. Loudes, et al. (1980). "Biosynthesis of precursor corticotropin/endorphin-, corticotropin-, alpha-melanotropin-, beta-lipotropin-, and beta-endorphin-like material by cultured neonatal rat hypothalamic neurons." Proc Natl Acad Sci U S A **77**(4): 1880-1884.

Ma, Y. C., W. J. Fan, et al. (2014). "Effect of Furin inhibitor on lung adenocarcinoma cell growth and metastasis." Cancer Cell Int **14**: 43.

Madani, R., S. Kozlov, et al. (2003). "Impaired explorative behavior and neophobia in genetically modified mice lacking or overexpressing the extracellular serine protease inhibitor neuroserpin." Mol Cell Neurosci **23**(3): 473-494.

Madani, R., S. Nef, et al. (2003). "Emotions are building up in the field of extracellular proteolysis." Trends Mol Med **9**(5): 183-185.

Magliery, T. J., C. G. Wilson, et al. (2005). "Detecting protein-protein interactions with a green fluorescent protein fragment reassembly trap: scope and mechanism." J Am Chem Soc **127**(1): 146-157.

Makarova, A., I. Mikhailenko, et al. (2003). "The low density lipoprotein receptor-related protein modulates protease activity in the brain by mediating the cellular internalization of both neuroserpin and neuroserpin-tissue-type plasminogen activator complexes." J Biol Chem **278**(50): 50250-50258.

Malide, D., N. G. Seidah, et al. (1995). "Electron microscopic immunocytochemical evidence for the involvement of the convertases PC1 and PC2 in the processing of proinsulin in pancreatic beta-cells." J Histochem Cytochem **43**(1): 11-19.

Marcinkiewicz, M. (2002). "BetaAPP and furin mRNA concentrates in immature senile plaques in the brain of Alzheimer patients." J Neuropathol Exp Neurol **61**(9): 815-829.

Marcinkiewicz, M., R. Day, et al. (1993). "Ontogeny of the prohormone convertases PC1 and PC2 in the mouse hypophysis and their colocalization with corticotropin and alpha-melanotropin." Proc Natl Acad Sci U S A **90**(11): 4922-4926.

Maret, D., M. S. Sadr, et al. (2012). "Opposite roles of furin and PC5A in N-cadherin processing." Neoplasia **14**(10): 880-892.

Mayer, G., G. Boileau, et al. (2004). "Sorting of furin in polarized epithelial and endothelial cells: expression beyond the Golgi apparatus." J Histochem Cytochem **52**(5): 567-579.

Melchor, J. P. and S. Strickland (2005). "Tissue plasminogen activator in central nervous system physiology and pathology." Thromb Haemost **93**(4): 655-660.

Miranda, E., K. Romisch, et al. (2004). "Mutants of neuroserpin that cause dementia accumulate as polymers within the endoplasmic reticulum." J Biol Chem **279**(27): 28283-28291.

Nagai, N., M. De Mol, et al. (1999). "Role of plasminogen system components in focal cerebral ischemic infarction: a gene targeting and gene transfer study in mice." Circulation **99**(18): 2440-2444.

Nagai, T. and K. Yamada (2008). "[Role of tissue plasminogen activator in the rewarding effect of nicotine]." Nihon Arukoru Yakubutsu Igakkai Zasshi **43**(3): 151-157.

Nagai, T., K. Yamada, et al. (2004). "The tissue plasminogen activator-plasmin system participates in the rewarding effect of morphine by regulating dopamine release." Proc Natl Acad Sci U S A **101**(10): 3650-3655.

Navarro-Yubero, C., A. Cuadrado, et al. (2004). "Neuroserpin is post-transcriptionally regulated by thyroid hormone." Brain Res Mol Brain Res **123**(1-2): 56-65.

Noto, R., M. G. Santangelo, et al. (2012). "The tempered polymerization of human neuroserpin." PLoS One **7**(3): e32444.

Nyfeler, B., S. W. Michnick, et al. (2005). "Capturing protein interactions in the secretory pathway of living cells." Proc Natl Acad Sci U S A **102**(18): 6350-6355.

Nyfeler, B., V. Reiterer, et al. (2008). "Identification of ERGIC-53 as an intracellular transport receptor of alpha1-antitrypsin." J Cell Biol **180**(4): 705-712.

Okano, H. J. and R. B. Darnell (1997). "A hierarchy of Hu RNA binding proteins in developing and adult neurons." J Neurosci **17**(9): 3024-3037.

Olson, S. T. and P. G. Gettins (2011). "Regulation of proteases by protein inhibitors of the serpin superfamily." Prog Mol Biol Transl Sci **99**: 185-240.

Orth, K., E. L. Madison, et al. (1992). "Complexes of tissue-type plasminogen activator and its serpin inhibitor plasminogen-activator inhibitor type 1 are internalized by means of the low density lipoprotein receptor-related protein/alpha 2-macroglobulin receptor." Proc Natl Acad Sci U S A **89**(16): 7422-7426.

Osterwalder, T., P. Cinelli, et al. (1998). "The axonally secreted serine proteinase inhibitor, neuroserpin, inhibits plasminogen activators and plasmin but not thrombin." J Biol Chem **273**(4): 2312-2321.

Osterwalder, T., J. Contartese, et al. (1996). "Neuroserpin, an axonally secreted serine protease inhibitor." EMBO J **15**(12): 2944-2953.

Osterwalder, T., A. Kuhnen, et al. (2004). "Drosophila serpin 4 functions as a neuroserpin-like inhibitor of subtilisin-like proprotein convertases." J Neurosci **24**(24): 5482-5491.

Parmar, P. K., L. C. Coates, et al. (2002). "Neuroserpin regulates neurite outgrowth in nerve growth factor-treated PC12 cells." J Neurochem **82**(6): 1406-1415.

Patston, P. A., P. Gettins, et al. (1991). "Mechanism of serpin action: evidence that C1 inhibitor functions as a suicide substrate." Biochemistry **30**(36): 8876-8882.

Pawlak, R., J. P. Melchor, et al. (2005). "Ethanol-withdrawal seizures are controlled by tissue plasminogen activator via modulation of NR2B-containing NMDA receptors." Proc Natl Acad Sci U S A **102**(2): 443-448.

Plaimauer, B., G. Mohr, et al. (2001). "'Shed' furin: mapping of the cleavage determinants and identification of its C-terminus." Biochem J **354**(Pt 3): 689-695.

Plotnick, M. I., M. Samakur, et al. (2002). "Heterogeneity in serpin-protease complexes as demonstrated by differences in the mechanism of complex breakdown." Biochemistry **41**(1): 334-342.

Qian, Z., M. E. Gilbert, et al. (1993). "Tissue-plasminogen activator is induced as an immediate-early gene during seizure, kindling and long-term potentiation." Nature **361**(6411): 453-457.

Raedler, T. J., M. B. Knable, et al. (1998). "Schizophrenia as a developmental disorder of the cerebral cortex." Curr Opin Neurobiol **8**(1): 157-161.

Raslan, A. and A. Bhardwaj (2007). "Medical management of cerebral edema." Neurosurg Focus **22**(5): E12.

Remy, I., A. Montmarquette, et al. (2004). "PKB/Akt modulates TGF-beta signalling through a direct interaction with Smad3." Nat Cell Biol **6**(4): 358-365.

Renatus, M., R. A. Engh, et al. (1997). "Lysine 156 promotes the anomalous proenzyme activity of tPA: X-ray crystal structure of single-chain human tPA." EMBO J **16**(16): 4797-4805.

Ricagno, S., S. Caccia, et al. (2009). "Human neuroserpin: structure and time-dependent inhibition." J Mol Biol **388**(1): 109-121.

Roebroek, A. J., L. Umans, et al. (1998). "Failure of ventral closure and axial rotation in embryos lacking the proprotein convertase Furin." Development **125**(24): 4863-4876.

Roet, K. C., E. H. Franssen, et al. (2013). "A multilevel screening strategy defines a molecular fingerprint of proregenerative olfactory ensheathing cells and identifies SCARB2, a protein that improves regenerative sprouting of injured sensory spinal axons." J Neurosci **33**(27): 11116-11135.

Rosnoblet, C., U. M. Vischer, et al. (1999). "Storage of tissue-type plasminogen activator in Weibel-Palade bodies of human endothelial cells." Arterioscler Thromb Vasc Biol **19**(7): 1796-1803.

Sarkar, A., C. Zhou, et al. (2011). "Local conformational flexibility provides a basis for facile polymer formation in human neuroserpin." Biophys J **101**(7): 1758-1765.

Sashindranath, M., E. Sales, et al. (2012). "The tissue-type plasminogen activator-plasminogen activator inhibitor 1 complex promotes neurovascular injury in brain trauma: evidence from mice and humans." Brain **135**(11): 3251-3264.

Scamuffa, N., F. Sfaxi, et al. (2014). "Prodomain of the proprotein convertase subtilisin/kexin Furin (ppFurin) protects from tumor progression and metastasis." Carcinogenesis **35**(3): 528-536.

Schipanski, A., F. Oberhauser, et al. (2014). "The lectin OS-9 delivers mutant neuroserpin to endoplasmic reticulum associated degradation in familial encephalopathy with neuroserpin inclusion bodies." Neurobiol Aging **35**(10): 2394-2403.

Schrimpf, S. P., A. J. Bleiker, et al. (1997). "Human neuroserpin (PI12): cDNA cloning and chromosomal localization to 3q26." Genomics **40**(1): 55-62.

Seidah, N. G. (2011). "The proprotein convertases, 20 years later." Methods Mol Biol **768**: 23-57.

Seidah, N. G. (2011). "What lies ahead for the proprotein convertases?" Ann N Y Acad Sci **1220**: 149-161.

Seidah, N. G., M. S. Sadr, et al. (2013). "The multifaceted proprotein convertases: their unique, redundant, complementary, and opposite functions." J Biol Chem **288**(30): 21473-21481.

Shen, F. S., N. G. Seidah, et al. (1993). "Biosynthesis of the prohormone convertase PC2 in Chinese hamster ovary cells and in rat insulinoma cells." J Biol Chem **268**(33): 24910-24915.

Shimomura, O., F. H. Johnson, et al. (1962). "Extraction, purification and properties of aequorin, a bioluminescent protein from the luminous hydromedusan, Aequorea." J Cell Comp Physiol **59**: 223-239.

Silverman, G. A., P. I. Bird, et al. (2001). "The serpins are an expanding superfamily of structurally similar but functionally diverse proteins. Evolution, mechanism of inhibition, novel functions, and a revised nomenclature." J Biol Chem **276**(36): 33293-33296.

Stefansson, S., S. Muhammad, et al. (1998). "Plasminogen activator inhibitor-1 contains a cryptic high affinity binding site for the low density lipoprotein receptor-related protein." J Biol Chem **273**(11): 6358-6366.

Stoeckli, E. T., P. F. Lemkin, et al. (1989). "Identification of proteins secreted from axons of embryonic dorsal-root-ganglia neurons." Eur J Biochem **180**(2): 249-258.

Sullivan, P. F., K. S. Kendler, et al. (2003). "Schizophrenia as a complex trait: evidence from a meta-analysis of twin studies." Arch Gen Psychiatry **60**(12): 1187-1192.

Takehara, S., M. Onda, et al. (2009). "The 2.1-A crystal structure of native neuroserpin reveals unique structural elements that contribute to conformational instability." J Mol Biol **388**(1): 11-20.

Taraska, J. W. and W. N. Zagotta (2010). "Fluorescence applications in molecular neurobiology." Neuron **66**(2): 170-189.

Tassew, N. G., J. Charish, et al. (2012). "SKI-1 and Furin generate multiple RGMa fragments that regulate axonal growth." Dev Cell **22**(2): 391-402.

Teesalu, T., A. Kulla, et al. (2004). "Tissue plasminogen activator and neuroserpin are widely expressed in the human central nervous system." Thromb Haemost **92**(2): 358-368.

Termini, J., J. Neman, et al. (2014). "Role of the Neural Niche in Brain Metastatic Cancer." Cancer Res **74**(15): 4011-4015.

Thimon, V., M. Belghazi, et al. (2006). "Analysis of furin ectodomain shedding in epididymal fluid of mammals: demonstration that shedding of furin occurs in vivo." Reproduction **132**(6): 899-908.

Thomas, G. (2002). "Furin at the cutting edge: from protein traffic to embryogenesis and disease." Nat Rev Mol Cell Biol **3**(10): 753-766.

Tranquille, N. and J. J. Emeis (1991). "On the role of calcium in the acute release of tissue-type plasminogen activator and von Willebrand factor from the rat perfused hindleg region." Thromb Haemost **66**(4): 479-483.

Tranquille, N. and J. J. Emeis (1993). "The role of cyclic nucleotides in the release of tissue-type plasminogen activator and von Willebrand factor." Thromb Haemost **69**(3): 259-261.

Tsang, V. W., D. Young, et al. (2014). "AAV-Mediated Overexpression of Neuroserpin in the Hippocampus Decreases PSD-95 Expression but Does Not Affect Hippocampal-Dependent Learning and Memory." PLoS One **9**(3): e91050.

Tsien, R. Y. (1998). "The green fluorescent protein." Annu Rev Biochem **67**: 509-544.

Tzimas, G. N., E. Chevet, et al. (2005). "Abnormal expression and processing of the proprotein convertases PC1 and PC2 in human colorectal liver metastases." BMC Cancer **5**: 149.

Valiente, M., A. C. Obenauf, et al. (2014). "Serpins promote cancer cell survival and vascular co-option in brain metastasis." Cell **156**(5): 1002-1016.

van Wamelen, D. J., N. A. Aziz, et al. (2013). "Decreased hypothalamic prohormone convertase expression in huntington disease patients." J Neuropathol Exp Neurol **72**(12): 1126-1134.

Wang, S. M., M. E. Ramsey, et al. (2014). "Plasticity of the mate choice mind: courtship evokes choice-like brain responses in females from a coercive mating system." Genes Brain Behav **13**(4): 365-375.

Wilson, C. G., T. J. Magliery, et al. (2004). "Detecting protein-protein interactions with GFP-fragment reassembly." Nat Methods **1**(3): 255-262.

Wong, R. Y., M. E. Ramsey, et al. (2012). "Localizing brain regions associated with female mate preference behavior in a swordtail." PLoS One **7**(11): e50355.

Wu, J., R. Echeverry, et al. (2010). "Neuroserpin protects neurons from ischemia-induced plasmin-mediated cell death independently of tissue-type plasminogen activator inhibition." Am J Pathol **177**(5): 2576-2584.

Yamada, M., K. Takahashi, et al. (2010). "Neuroserpin is expressed in early stage of neurogenesis in adult rat hippocampus." Neuroreport **21**(2): 138-142.

Yamasaki, M., W. Li, et al. (2008). "Crystal structure of a stable dimer reveals the molecular basis of serpin polymerization." Nature **455**(7217): 1255-1258.

Yazaki, M., J. J. Liepnieks, et al. (2001). "Biochemical characterization of a neuroserpin variant associated with hereditary dementia." Am J Pathol **158**(1): 227-233.

Yepes, M., M. Sandkvist, et al. (2002). "Regulation of seizure spreading by neuroserpin and tissue-type plasminogen activator is plasminogen-independent." J Clin Invest **109**(12): 1571-1578.

Yepes, M., M. Sandkvist, et al. (2000). "Neuroserpin reduces cerebral infarct volume and protects neurons from ischemia-induced apoptosis." Blood **96**(2): 569-576.

Zhang, Z., L. Zhang, et al. (2002). "Adjuvant treatment with neuroserpin increases the therapeutic window for tissue-type plasminogen activator administration in a rat model of embolic stroke." Circulation **106**(6): 740-745.

Zheng, M., R. D. Streck, et al. (1994). "The developmental expression in rat of proteases furin, PC1, PC2, and carboxypeptidase E: implications for early maturation of proteolytic processing capacity." J Neurosci **14**(8): 4656-4673.

Zhou, Z., R. Wang, et al. (2014). "The cAMP-responsive element binding protein (CREB) transcription factor regulates furin expression during human trophoblast syncytialization." Placenta **35**(11): 907-918.

Zimmer, M. (2009). "GFP: from jellyfish to the Nobel prize and beyond." Chem Soc Rev **38**(10): 2823-2832.

8 Acknowledgments

9 Curriculum vitae

PERSONAL DATA

Name:	Felix Johannes Alfred Wiesmueller
Date/place of birth:	10-25-1985 in Regensburg, Germany
Address:	Emil-Andresen-Strasse 5; 22529 Hamburg, Germany
Phone/email:	+49-162-4763098; f.wiesmueller@gmx.de

EDUCATION

2008 - present:	**Universität Hamburg**, Hamburg, Germany;
2007-2008:	**Università degli studi di Padova,** Padova, Italy; "Chimica e Tecnologia farmaceutiche".
1996-2006:	**Musikgymnasium der Regensburger Domspatzen,** Regensburg, Germany; Degree: Abitur (1,9)
2003-2004:	**Madison County High School,** Madison FL, USA; Degree: Honorary Diploma

FINAL YEAR ELECTIVES

April 2014 – July 2014:	**Neurology**; Klinikum Itzehoe, Germany.
December 2013 – April 2014:	**Surgery**; Asklepios Klinik St. Georg, Hamburg, Germany.
August 2013 – December 2013:	**Internal Medicine**; Klinikum Itzehoe, Germany.

ELECTIVE CLERKSHIPS

July 2013 – August 2013:	**Neurosurgery**; Asklepios Klinik Altona, Hamburg, Germany.
August 2012:	**Neuropathology**; University Medical Center Hamburg-Eppendorf, Germany.
September 2011:	**Emergency Medicine**; University Hospital Regensburg, Germany.
July 2011 - August 2011:	**Plastic and Aesthetic, Hand- and Reconstructive Surgery**; Caritas-Hospital St. Josef, Regensburg, Germany.

SCHOLARSHIPS

2003-2004:	**Congress-Bundestag Youth Exchange Program (CBYX) Scholarship.**

EMPLOYMENT

December 2011 – April 2014:	**Asklepios Klinik St. Georg, Hamburg**. Student assistant.
February 2009 - March 2012:	**Endo-Klinik, Hamburg.** Student assistant.

10 Eidesstattliche Versicherung *[als letztes Blatt in die Dissertation einzubinden]*

Ich versichere ausdrücklich, dass ich die Arbeit selbständig und ohne fremde Hilfe verfasst, andere als die von mir angegebenen Quellen und Hilfsmittel nicht benutzt und die aus den benutzten Werken wörtlich oder inhaltlich entnommenen Stellen einzeln nach Ausgabe (Auflage und Jahr des Erscheinens), Band und Seite des benutzten Werkes kenntlich gemacht habe.
Ferner versichere ich, dass ich die Dissertation bisher nicht einem Fachvertreter an einer anderen Hochschule zur Überprüfung vorgelegt oder mich anderweitig um Zulassung zur Promotion beworben habe.
Ich erkläre mich einverstanden, dass meine Dissertation vom Dekanat der Medizinischen Fakultät mit einer gängigen Software zur Erkennung von Plagiaten überprüft werden kann.

Unterschrift: ....